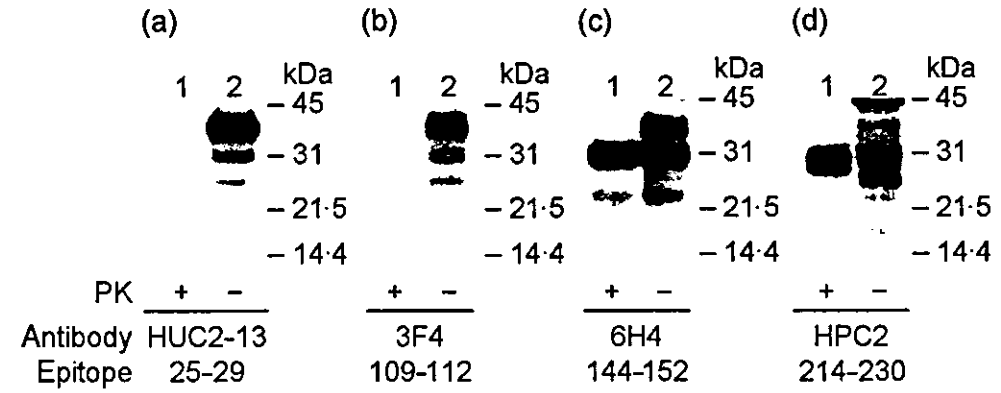

Fig. 3. Immunoblot analysis using anti-PrP antibodies for the protease-resistant form of PrP in T98G cells. T98G cells were incubated with 10% FCS/RPMI 1640 for 40 days after 40 passages (P40D40); whole-cell, methanol-precipitated lysates were treated with PK (lane 1) or left undigested (lane 2). PK-treated lysates were subjected to immunoblot with the HUC2-13 (a), 3F4 (b), 6H4 (c) or HPC2 (d) antibodies as described in Methods. Epitope recognition sites located within PrP are shown as amino acid numbers.

by indirect immunofluorescence staining. Immunoreactive PrP with 6H4 antibody was observed on the cell surface as a bright fluorescent signal (Fig. 4a), whereas little signal was observed with mouse IgG, a control antibody purified from normal mouse serum (data not shown). We next prepared membrane and cytosolic fractions from homogenates of P40D40 T98G cells and measured the amount of PrP by competitive ELISA using the 6H4 antibody. PrP was recovered predominantly in the membrane fraction (Table 1). As shown in Fig. 4b, the distribution of PrP^{res} in P40D40 T98G cells (left panel) was similar to that of PrP^{C} in P3D36 T98G cells (right panel); PrP^{res} was detected in the membrane fraction (left panel, lane 3), as well as in homogenates (left panel, lane 1), but no PrP was detected in the cytosolic fraction (left panel, lanes 5 and 6). These data indicated that most PrP^{res} was in the membrane fraction, probably on the plasma membrane. To test the detergent solubility of PrP, the homogenates of P40D40 T98G cells were centrifuged in non-ionic detergents. A large proportion of immunoreactive PrP was found in the supernatant fraction (Fig. 4c, lane 3), but no PrP was detected in the pellet fraction (Fig. 4c, lane 2). These

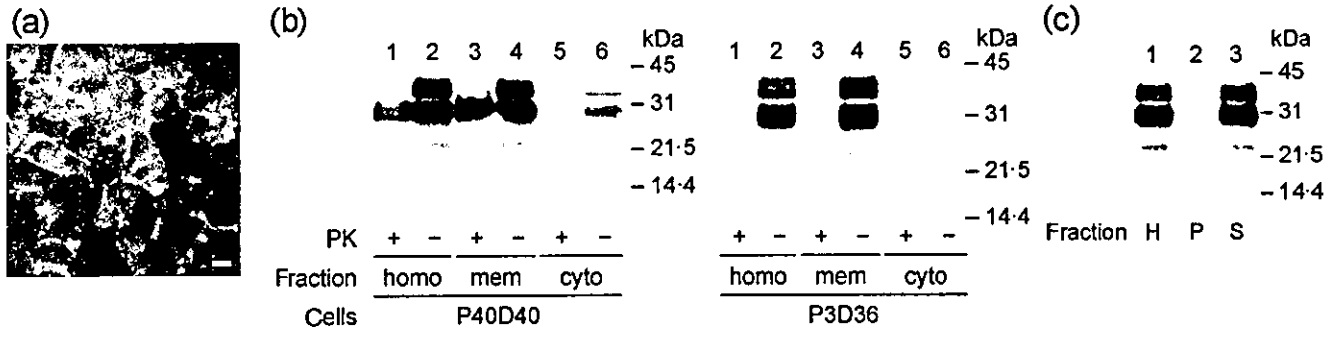

Fig. 4. Subcellular localization and detergent solubility of PrP^{res} in long-term cultured T98G cells. T98G cells were incubated with 10% FCS/RPMI 1640 in the long-term incubation after repeated passages. (a) T98G cells for 40 days after 40 passages (P40D40) on a 15 mm glass coverslip were subjected to indirect immunofluorescence staining with the 6H4 antibody as described in Methods. Bar, 10 μm. (b) T98G cells for 40 days after 40 passages (P40D40, left panel) and for 36 days after 3 passages (P3D36, right panel) were scraped into PBS/2·5 mM EDTA and sonicated. Homogenates (homo) were separated into a membrane fraction (mem) and a cytosolic fraction (cyto). Methanol-precipitated lysates were treated with PK (lanes 1, 3 and 5) or left undigested (lanes 2, 4 and 6). PK-treated samples were subjected to immunoblotting with the 6H4 antibody as described in Methods. (c) T98G cells for 40 days after 40 passages (P40D40) were scraped into PBS/2·5 mM EDTA and sonicated. Homogenates (H) of 50 μg protein were centrifuged as described in Methods to obtain a non-ionic detergent-insoluble pellet (P) and a soluble supernatant fraction (S). Homogenates, pellet and supernatant fractions (50 μg protein each) were subjected to immunoblot with the 6H4 antibody as described in Methods.

Table 1. Subcellular localization of PrP in long-term cultured T98G cells

The amount of PrP is expressed as recombinant bovine PrP equivalents per 10^7 cells. Values are means ± SEM ($n=4$).

Sample	PrP content	
	pmol	%
Homogenate	263·4 ± 20·9	100·0
Membrane fraction	228·9 ± 17·5	86·9
Cytosolic fraction	9·9 ± 0·5	3·8

experiments indicated that PrP^{res} in T98G cells was non-ionic detergent-soluble.

DISCUSSION

The mechanism of the conversion of PrP has not been studied in human cell cultures, due to the lack of a model system. In the present study, we developed such a system by culturing human glioblastoma T98G cells, which express endogenous PrP^{C} constitutively. After reaching a high passage number, long-term cultured T98G cells converted PrP^{C} into PrP^{res}.

Direct sequencing of amplified *PRNP* mRNA and RFLP analysis indicated that the T98G cells were heterozygotes at codon 129 (129M/V) and that no new coding mutations were present in cells that had been subjected to long-term cultures. The deglycosylated form of PK-treated PrP^{res} in T98G cells migrated at approximately 18 kDa. In human prion diseases, two major types of PrP^{res} can be identified, based on electrophoretic migration; the relative molecular mass of the unglycosylated form is approximately 21 kDa (described as type 1) or 19 kDa (described as type 2) (Parchi *et al.*, 1997). Accordingly, PrP^{res} in T98G cells is similar to the previously described MV2 phenotypic variant (Parchi *et al.*, 1999a). However, the size of the deglycosylated PK-resistant fragment in T98G cells was smaller than that of the corresponding fragments observed in type 2 PrP^{res}. Most importantly, the 3F4 antibody, which is a well-characterized antibody known to target residues 109–112 as its epitope (Kascsak *et al.*, 1987; Matsunaga *et al.*, 2001), did not react with PK-digested PrP^{res} in T98G cells, suggesting that the N-terminal PrP region up to residue 109 might be absent in PK-treated PrP^{res} in T98G cells. Human PrP^{res} peptide is divided into three regions that are defined by their PK-cleavage patterns: an N-terminal region (residues 23–73) that is invariably PK-sensitive, a C-terminal region (residues 103–231) that is invariably PK-resistant and a variably digested region (residues 74–102), where the major cleavage sites are at G82 in type 1 and at S97 in type 2 (Parchi *et al.*, 2000). The 3F4 antibody was used to type PrP^{res} (Parchi *et al.*, 2000). Therefore, there are striking differences in the antigenicity, which reflect the PK-cleavage patterns, between type 2 PrP^{res} in sporadic CJD brain and in T98G cells. It is unlikely, but not impossible, that PK treatment generated conformational changes in the mid-region of PrP^{res} that interfered with epitope recognition by the 3F4 antibody. Further studies are needed to classify the type of PrP^{res} in lysates from long-term cultured T98G cells.

So far, human PrP^{Sc} has been analysed on immunoblots with the 3F4 antibody. Our finding may explain why previous studies have failed to detect PrP^{res} in cultured cells. Interestingly, an N-terminally truncated 18 kDa fragment of PrP (designated C1) in normal and sporadic CJD brains has similar properties except that it is PK-sensitive; it is recognized by the anti-C terminus antibody, but not by the 3F4 antibody, is cleaved around residue 111 and is associated with cell membranes (Chen *et al.*, 1995). PrP^{C} from human brain homogenates ($n=6$) originally displayed a partial PK resistance (20 μg ml^{-1} for 10 min) and has been detected by the antibody that recognizes residues 145–163, but not by the 3F4 antibody (Buschmann *et al.*, 1998). Taking the data from the various studies of PrP immunoreactivity into consideration, we believe that it would be better to incorporate an additional antibody that recognizes the C terminus of PrP into the standardly used protease resistance-dependent PrP^{Sc} assay.

Among the sets of antibodies used in this study, the anti-N-terminal portion antibodies (HUC2-13 and 3F4) reacted strongly with the fully glycosylated form and moderately with the partially glycosylated form. In contrast, the antibodies against the C-terminal portion of PrP (6H4 and HPC) reacted moderately with the fully glycosylated form and strongly with the partially glycosylated form. It is possible that PK digestion induces a conformational change of digested PrP and enhances its immunoreactivity to the anti-C-terminal antibodies. Recently, it has been reported that the amino acid motif Tyr-Tyr-Arg (YYR), located in a β-sheet, is exposed in PrP^{Sc}, whilst it is cryptic in PrP^{C}, and that antibodies recognize YYR in PrP^{Sc}, but not in PrP^{C} (Paramithiotis *et al.*, 2003). Another paper has reported that PK digestion enhances immunoreactivity to the anti-PrP antibody that recognizes the epitope YYR, located in a β-sheet (Brun *et al.*, 2004). These reports suggest that conformation of the C-terminal portion of PrP^{Sc} is essential for immunoreactivity of anti-YYR antibodies. The 6H4 antibody also recognizes residues 144–152 of PrP, including a YYR motif that is located in an α-helix, not in a β-sheet (Korth *et al.*, 1997). Further study is needed to clarify the immunoreactivity of anti-C-terminal PrP antibodies.

It has been proposed that PrP^{C} is converted into PrP^{res} either on the cell surface or in endocytic cellular compartments. PrP^{C} is a surface protein that contains a glycosylphosphatidylinositol anchor (Stahl *et al.*, 1987). A portion of PrP^{Sc} is also localized on the cell surface of scrapie-infected mouse neuroblastoma ScN2a cells (Naslavsky *et al.*, 1997; Vey *et al.*, 1996), although it is also found in lysosomes (Taraboulos *et al.*, 1990). Subcellular localization of PrP^{res} in long-term cultured T98G cells was similar to that of PrP^{Sc}-infected cells, being present on the cell surface.

PrP^{Sc} in ScN2a cells is sedimented by centrifugation in non-ionic detergents (Caughey *et al.*, 1991). Mutant PrP in stably transfected Chinese hamster ovary cells, which express murine homologues associated with human inherited prion diseases, is also non-ionic detergent-insoluble (Lehmann & Harris, 1996). However, the PrP^{res} in T98G cells is detergent-soluble. PrP^{res} in the human neuroblastoma cell line M-17 BE(2)C carrying the familial subtype CJD, the glutamic acid to lysine substitution at codon 200 (E200K), is also partially non-ionic detergent-insoluble (Capellari *et al.*, 2000). The present study indicates that not all PrP^{res} is non-ionic detergent-insoluble.

Many cultured cells that express PrP^{res} mutants carrying substitutions of inherited prion disease show considerably less protease resistance (up to 3·3 μg ml^{-1} for 10 min), compared with PrP^{res} mutants isolated from the human brain (Capellari *et al.*, 2000; Harris, 2001). In contrast, the PrP^{res} in T98G cells displayed a high resistance to digestion with PK (10 μg ml^{-1} for 30 min), but was less resistant than PrP^{res} in brain homogenates of sporadic CJD (up to 100 μg ml^{-1} for 24 h). Sporadic CJD is typically characterized by widespread spongiform degeneration with loss of neurons, gliosis and formation of amyloid plaques (Parchi *et al.*, 1999a). It has recently been reported that six cases of sporadic fatal insomnia, a prion disease mimicking fatal familial insomnia, had no coding-region mutation of *PRNP* with the 129 M/M genotype and an approximately 19 kDa deglycosylated PrP^{res}, the same as that of type 2 (Mastrianni *et al.*, 1999; Parchi *et al.*, 1999b). Familial progressive subcortical gliosis may also be a prion disease, characterized by astrogliosis at the cortex–white matter junction (Petersen *et al.*, 1995). All patients from two families with that disease showed no coding-region mutation of *PRNP*, the 129 M/M genotype and the 18·1–19·3 kDa form of deglycosylated PrP^{res} (Petersen *et al.*, 1995). T98G cells were grown out of human glioblastoma multiforma tumour tissue of a 61-year-old Caucasian man (Stein, 1979). We consider it possible that he also had a sporadic form of prion disease.

Conversion from PrP^{C} into PrP^{res} is an important process, because most prion diseases are characterized by presence of PrP^{res}. Some knowledge of the conversion mechanism is based on studies of scrapie-infected cells. Recently, it has been reported that several conditions can induce the formation of PrP^{res} in cultured cells. Proteasome inhibitors cause accumulation of the unglycosylated form of PrP^{res} in treated cells (Lehmann & Harris, 1997; Ma & Lindquist, 1999; Yedidia *et al.*, 2001). PrP that misfolds during maturation in the endoplasmic reticulum is delivered to the cytosol for degradation by proteasomes (Béranger *et al.*, 2002; Ma & Lindquist, 2001; Yedidia *et al.*, 2001). It has been hypothesized the conversion into PrP^{res} might occur when the number of PrP molecules exceeds the capacity of the cell to degrade them (Ma & Lindquist, 2002). Another study showed that manganese-treated mouse astrocytes express the glycosylated form of PrP^{res} (Brown *et al.*, 2000).

Here, we report for the first time the conversion of PrP^{C} into PrP^{res} in the widely used human glioblastoma cell line T98G; a large number of passages and prolonged incubation under routine cell-culture conditions are required. *In vitro*-generated PrP^{res} is reportedly not sufficient for the production of infectivity (Caughey *et al.*, 2001; Hill *et al.*, 1999) and further study is needed to clarify the infectivity of PrP^{res} in T98G cells (indeed, caution should be taken with T98G cells in the laboratory). Infectivity assays of PrP^{res} in T98G cells are now in progress in transgenic mice.

In conclusion, T98G cells should be a useful model for studying the mechanisms of PrP^{C} conversion into PrP^{res}.

ACKNOWLEDGEMENTS

This work was supported by grants from Research on Hepatitis and BSE (H14-BSE-002) and Risk Analysis Research on Food and Pharmaceuticals (H14-BSE-001 and 003) from the Ministry of Health, Labor and Welfare, Japan.

REFERENCES

Archer, F., Bachelin, C., Andreoletti, O. & 8 other authors (2004). Cultured peripheral neuroglial cells are highly permissive to sheep prion infection. *J Virol* **78**, 482–490.

Béranger, F., Mangé, A., Goud, B. & Lehmann, S. (2002). Stimulation of PrP^{C} retrograde transport toward the endoplasmic reticulum increases accumulation of PrP^{Sc} in prion-infected cells. *J Biol Chem* **277**, 38972–38977.

Birkett, C. R., Hennion, R. M., Bembridge, D. A., Clarke, M. C., Chree, A., Bruce, M. E. & Bostock, C. J. (2001). Scrapie strains maintain biological phenotypes on propagation in a cell line in culture. *EMBO J* **20**, 3351–3358.

Brown, D. R., Hafiz, F., Glasssmith, L. L., Wong, B.-S., Jones, I. M., Clive, C. & Haswell, S. J. (2000). Consequences of manganese replacement of copper for prion protein function and proteinase resistance. *EMBO J* **19**, 1180–1186.

Brun, A., Castilla, J., Ramírez, M. A. & 8 other authors (2004). Proteinase K enhanced immunoreactivity of the prion protein-specific monoclonal antibody 2A11. *Neurosci Res* **48**, 75–83.

Buschmann, A., Kuczius, T., Bodemer, W. & Groschup, M. H. (1998). Cellular prion proteins of mammalian species display an intrinsic partial proteinase K resistance. *Biochem Biophys Res Commun* **253**, 693–702.

Butler, D. A., Scott, M. R. D., Bockman, J. M., Borchelt, D. R., Taraboulos, A., Hsiao, K. K., Kingsbury, D. T. & Prusiner, S. B. (1988). Scrapie-infected murine neuroblastoma cells produce protease-resistant prion proteins. *J Virol* **62**, 1558–1564.

Capellari, S., Parchi, P., Russo, C. M., Sanford, J., Sy, M. S., Gambetti, P. & Petersen, R. B. (2000). Effect of the E200K mutation on prion protein metabolism. Comparative study of a cell model and human brain. *Am J Pathol* **157**, 613–622.

Caughey, B. & Raymond, G. J. (1993). Sulfated polyanion inhibition of scrapie-associated PrP accumulation in cultured cells. *J Virol* **67**, 643–650.

Caughey, B., Raymond, G. J., Ernst, D. & Race, R. E. (1991). N-terminal truncation of the scrapie-associated form of PrP by lysosomal protease(s): implications regarding the site of conversion of PrP to the protease-resistant state. *J Virol* **65**, 6597–6603.

Caughey, B., Horiuchi, M., Demaimay, R. & Raymond, G. J. (1999). Assays of protease-resistant prion protein and its formation. *Methods Enzymol* **309**, 122–133.

Caughey, B., Raymond, G. J., Callahan, M. A., Wong, C., Baron, G. S. & Xiong, L.-W. (2001). Interactions and conversions of prion protein isoforms. *Adv Protein Chem* **57**, 139–169.

Chen, S. G., Teplow, D. B., Parchi, P., Teller, J. K., Gambetti, P. & Autilio-Gambetti, L. (1995). Truncated forms of the human prion protein in normal brain and in prion diseases. *J Biol Chem* **270**, 19173–19180.

Clarke, M. C. & Haig, D. A. (1970). Evidence for the multiplication of scrapie agent in cell culture. *Nature* **225**, 100–101.

Doh-Ura, K., Iwaki, T. & Caughey, B. (2000). Lysosomotropic agents and cysteine protease inhibitors inhibit scrapie-associated prion protein accumulation. *J Virol* **74**, 4894–4897.

Follet, J., Lemaire-Vieille, C., Blanquet-Grossard, F. & 8 other authors (2002). PrP expression and replication by Schwann cells: implications in prion spreading. *J Virol* **76**, 2434–2439.

Harris, D. A. (2001). Biosynthesis and cellular processing of the prion protein. *Adv Protein Chem* **57**, 203–228.

Hill, A. F., Antoniou, M. & Collinge, J. (1999). Protease-resistant prion protein produced *in vitro* lacks detectable infectivity. *J Gen Virol* **80**, 11–14.

Kascsak, R. J., Rubenstein, R., Merz, P. A., Tonna-DeMasi, M., Fersko, R., Carp, R. I., Wisniewski, H. M. & Diringer, H. (1987). Mouse polyclonal and monoclonal antibody to scrapie-associated fibril proteins. *J Virol* **61**, 3688–3693.

Kikuchi, Y., Irie, M., Yoshimatsu, K. & 8 other authors (1991). A monoclonal antibody to scopolamine and its use for competitive enzyme-linked immunosorbent assay. *Phytochemistry* **30**, 3273–3276.

Kikuchi, Y., Kakeya, T., Yamazaki, T. & 7 other authors (2002). G_1-dependent prion protein expression in human glioblastoma cell line T98G. *Biol Pharm Bull* **25**, 728–733.

Korth, C., Stierli, B., Streit, P. & 14 other authors (1997). Prion (PrP^{Sc})-specific epitope defined by a monoclonal antibody. *Nature* **390**, 74–77.

Kovács, G. G., Trabattoni, G., Hainfellner, J. A., Ironside, J. W., Knight, R. S. G. & Budka, H. (2002). Mutations of the prion protein gene phenotypic spectrum. *J Neurol* **249**, 1567–1582.

Ladogana, A., Liu, Q., Xi, Y. G. & Pocchiari, M. (1995). Proteinase-resistant protein in human neuroblastoma cells infected with brain material from Creutzfeldt-Jakob patient. *Lancet* **345**, 594–595.

Lehmann, S. & Harris, D. A. (1996). Mutant and infectious prion proteins display common biochemical properties in cultured cells. *J Biol Chem* **271**, 1633–1637.

Lehmann, S. & Harris, D. A. (1997). Blockade of glycosylation promotes acquisition of scrapie-like properties by the prion protein in cultured cells. *J Biol Chem* **272**, 21479–21487.

Ma, J. & Lindquist, S. (1999). De novo generation of a PrP^{Sc}-like conformation in living cells. *Nat Cell Biol* **1**, 358–361.

Ma, J. & Lindquist, S. (2001). Wild-type PrP and a mutant associated with prion disease are subject to retrograde transport and proteasome degradation. *Proc Natl Acad Sci U S A* **98**, 14955–14960.

Ma, J. & Lindquist, S. (2002). Conversion of PrP to a self-perpetuating PrP^{Sc}-like conformation in the cytosol. *Science* **298**, 1785–1788.

Mastrianni, J. A., Nixon, R., Layzer, R., Telling, G. C., Han, D., DeArmond, S. J. & Prusiner, S. B. (1999). Prion protein conformation in a patient with sporadic fatal insomnia. *N Engl J Med* **340**, 1630–1638.

Matsuda, H., Mitsuda, H., Nakamura, N., Furusawa, S., Mohri, S. & Kitamoto, T. (1999). A chicken monoclonal antibody with specificity for the N-terminal of human prion protein. *FEMS Immunol Med Microbiol* **23**, 189–194.

Matsunaga, Y., Peretz, D., Williamson, A., Burton, D., Mehlhorn, I., Groth, D., Cohen, F. E., Prusiner, S. B. & Baldwin, M. A. (2001). Cryptic epitopes in N-terminally truncated prion protein are exposed in the full-length molecule: dependence of conformation on pH. *Proteins* **44**, 110–118.

Moser, M., Colello, R. J., Pott, U. & Oesch, B. (1995). Developmental expression of the prion protein gene in glial cells. *Neuron* **14**, 509–517.

Naslavsky, N., Stein, R., Yanai, A., Friedlander, G. & Taraboulos, A. (1997). Characterization of detergent-insoluble complexes containing the cellular prion protein and its scrapie isoform. *J Biol Chem* **272**, 6324–6331.

Nishida, N., Harris, D. A., Vilette, D., Laude, H., Frobert, Y., Grassi, J., Casanova, D., Milhavet, O. & Lehmann, S. (2000). Successful transmission of three mouse-adapted scrapie strains to murine neuroblastoma cell lines overexpressing wild-type mouse prion protein. *J Virol* **74**, 320–325.

Paramithiotis, E., Pinard, M., Lawton, T. & 19 other authors (2003). A prion protein epitope selective for the pathologically misfolded conformation. *Nat Med* **9**, 893–899.

Parchi, P., Capellari, S., Chen, S. G. & 8 other authors (1997). Typing prion isoforms. *Nature* **386**, 232–234.

Parchi, P., Giese, A., Capellari, S. & 15 other authors (1999a). Classification of sporadic Creutzfeldt-Jakob disease based on molecular and phenotypic analysis of 300 subjects. *Ann Neurol* **46**, 224–233.

Parchi, P., Capellari, S., Chin, S. & 7 other authors (1999b). A subtype of sporadic prion disease mimicking fatal familial insomnia. *Neurology* **52**, 1757–1763.

Parchi, P., Zou, W., Wang, W. & 10 other authors (2000). Genetic influence on the structural variations of the abnormal prion protein. *Proc Natl Acad Sci U S A* **97**, 10168–10172.

Petersen, R. B., Tabaton, M., Chen, S. G. & 10 other authors (1995). Familial progressive subcortical gliosis: presence of prions and linkage to chromosome 17. *Neurology* **45**, 1062–1067.

Prusiner, S. B. (2001). Prions. In *Fields Virology*, 4th edn, pp. 3063–3087. Edited by D. M. Knipe & P. M. Howley. Philadelphia, PA: Lippincott Williams & Wilkins.

Race, R. E., Fadness, L. H. & Chesebro, B. (1987). Characterization of scrapie infection in mouse neuroblastoma cells. *J Gen Virol* **68**, 1391–1399.

Rubenstein, R., Carp, R. I. & Callahan, S. M. (1984). *In vitro* replication of scrapie agent in a neuronal model: infection of PC12 cells. *J Gen Virol* **65**, 2191–2198.

Satoh, J., Kurohara, K., Yukitake, M. & Kuroda, Y. (1998). Constitutive and cytokine-inducible expression of prion protein gene in human neural cell lines. *J Neuropathol Exp Neurol* **57**, 131–139.

Schätzl, H. M., Laszlo, L., Holtzman, D. M., Tatzelt, J., DeArmond, S. J., Weiner, R. I., Mobley, W. C. & Prusiner, S. B. (1997). A hypothalamic neuronal cell line persistently infected with scrapie prions exhibits apoptosis. *J Virol* **71**, 8821–8831.

Stahl, N., Borchelt, D. R., Hsiao, K. & Prusiner, S. B. (1987). Scrapie prion protein contains a phosphatidylinositol glycolipid. *Cell* **51**, 229–240.

Stein, G. H. (1979). T98G: an anchorage-independent human tumor cell line that exhibits stationary phase G_1 arrest in vitro. *J Cell Physiol* **99**, 43–54.

Takekida, K., Kikuchi, Y., Yamazaki, T. & 7 other authors (2002). Quantitative analysis of prion protein by immunoblotting. *J Health Sci* **48**, 288–291.

Taraboulos, A., Serban, D. & Prusiner, S. B. (1990). Scrapie prion proteins accumulate in the cytoplasm of persistently infected cultured cells. *J Cell Biol* **110**, 2117–2132.

van Keulen, L. J., Schreuder, B. E., Meloen, R. H., Poelen-van den Berg, M., Mooij-Harkes, G., Vromans, M. E. & Langeveld, J. P. (1995). Immunohistochemical detection and localization of prion protein in brain tissue of sheep with natural scrapie. *Vet Pathol* **32**, 299–308.

Vey, M., Pilkuhn, S., Wille, H., Nixon, R., DeArmond, S. J., Smart, E. J., Anderson, R. G. W., Taraboulos, A. & Prusiner, S. B. (1996). Subcellular colocalization of the cellular and scrapie prion proteins in caveolae-like membranous domains. *Proc Natl Acad Sci U S A* **93**, 14945–14949.

Yedidia, Y., Horonchik, L., Tzaban, S., Yanai, A. & Taraboulos, A. (2001). Proteasomes and ubiquitin are involved in the turnover of the wild-type prion protein. *EMBO J* **20**, 5383–5391.

Acta Neuropathologica

10.1007/s00401-004-0944-x

Regular Paper

Effective antigen-retrieval method for immunohistochemical detection of abnormal isoform of prion proteins in animals

Hidefumi Furuoka[1] ✉, Atushi Yabuzoe[1], Motohiro Horiuchi[2, 3], Yuichi Tagawa[4], Takashi Yokoyama[4], Yoshio Yamakawa[5], Morikazu Shinagawa[4] and Tetsutaro Sata[6]

(1) Department of Pathobiological Science, Obihiro University of Agriculture and Veterinary Medicine, 080-8555 Obihiro, Japan
(2) Department of Applied Veterinary Science, Obihiro University of Agriculture and Veterinary Medicine, 080-8555 Obihiro, Japan
(3) Research Center for Protozoan Diseases, Obihiro University of Agriculture and Veterinary Medicine, 080-8555 Obihiro, Japan
(4) Prion Disease Research Center, National Institute of Animal Health, 305-0856 Ibaraki, Japan
(5) Department of Biochemistry and Cell Biology, National Institute of Infectious Diseases, 162-8640 Tokyo, Japan
(6) Department of Pathology, National Institute of Infectious Diseases, 162-8640 Tokyo, Japan

✉ **Hidefumi Furuoka**
Email: furuoka@obihiro.ac.jp
Fax: +81-155-495364

Received: 12 July 2004 **Revised:** 12 October 2004 **Accepted:** 12 October 2004 **Published online:** 22 December 2004

Abstract For immunohistochemistry of the prion diseases, several pretreatment methods to enhance the immunoreactivity of human and animal abnormal proteinase-resistant prion protein (PrP^{Sc}) on the tissue sections have been employed. The method of 121°C hydrated autoclaving pretreatment or the combination method of 121°C hydrated autoclaving with a certain chemical reagent (formic acid or proteinase K, etc) are now widely used. We found that an improved hydrated autoclaving method at 135°C, more effectively enhanced PrP^{Sc} immunoreactivity for the antibodies recognizing the linear epitope. In addition, this method was more effective for the long-term fixation samples as compared with other previous methods. However, this modified method could not retrieve PrP^{Sc} antigenic epitopes composed of conformational structures or several discontinuous epitopes. We describe the comparative studies between our improved method and other antigen-retrieval procedures reported previously. Based on the differences of reaction among the antibodies, we also discuss the mechanisms of the hydrated autoclaving methods to retrieve PrP^{Sc} immunoreactivity.

Keywords Prion protein - Immunohistochemistry - Antigen retrieval - Autoclaving - Monoclonal antibody

Introduction

Scrapie in sheep and goat, bovine spongiform encephalopathy (BSE), chronic wasting disease in deer and Creutzfeldt-Jakob disease (sporadic, iatrogenic, familial and variant forms) and Kuru in humans are transmissible neurodegenerative disorders belonging to a group of prion diseases. They are characterized by the accumulation of abnormal proteinase-resistant prion protein (PrP^{Sc}), which is an isoform of the cellular, proteinase-sensitive prion protein (PrP^{C}), as a result of post-translational modification with increases of the population of β-sheet conformation in the brain [20]. The pathology is characterized by neuronal cell loss, spongiform change, gliosis and deposition of abnormal amyloid protein.

Immunohistochemistry to demonstrate PrP^{Sc} in tissue sections is now a well-established technique for the diagnosis of prion diseases [2]. It has been reported that PrP^{Sc} immunoreactivity is enhanced by several antigen-retrieval procedures such as formic acid [4, 10], a combination of formic acid pretreatment and microwave processing [7, 14], hydrated or hydrolytic autoclaving [6, 11], guanidine thiocyanate [4, 19], and combined protocols [1, 8, 9, 15].

The recent disclosure of BSE in Japan has started an active surveillance for all slaughter cattle since October 2001. Briefly, diagnostic procedure is follows: samples have been taken from the medulla oblongata (obex region) and examined by ELISA as the primary screening test; the ELISA-positive samples have then been confirmed by Western blot and/or immunohistochemistry. In starting an active surveillance for BSE in Japan, we applied various pretreatment methods for different antibodies to formalin-fixed and paraffin-embedded tissues to enhance PrP^{Sc} immunoreactivity. Although the pretreatment methods reported previously were found to retrieve PrP^{Sc} for antibodies used in this study, we found that an improved hydrated autoclaving method at 135°C more effectively enhanced PrP^{Sc} immunoreactivity for the antibodies recognizing the linear epitope. However, our modified method could not retrieve PrP^{Sc} antigens well for the monoclonal antibodies recognizing the conformational structures.

Here we describe the comparative studies between our improved method and other antigen-retrieval procedures reported previously, and discuss the mechanisms of the hydrated autoclaving methods to retrieve PrP^{Sc} immunoreactivity.

Materials and methods

Samples

We used the brain tissues that were cut coronally at the level including hippocampus and thalamus from two scrapie-infected and two negative control ICR mice, the medulla oblongata at the level of the obex, and the spinal cord from three scrapie-affected and two negative control sheep, and from three BSE-affected cattle in Japan and two control cattle. Two mice were inoculated intracerebrally with scrapie G1 strain, which induces amyloid plaque formations in the brain. Affected or non-affected sheep and cattle were diagnosed and confirmed by histological, immunohistochemical, and Western blot methods. These samples were fixed in 15% formalin for 48–72 h and embedded routinely in paraffin. BSE tissue blocks were treated with 98% formic acid for 1 h to reduce the infectivity of prion after formalin fixation. In addition, we prepared the serial tissue blocks from the medulla oblongata of scrapie-affected sheep, which was immersed in 15% formalin at least for 6 months.

Immunohistochemistry

Serial tissue sections, 4 μm in thickness, were picked up on silane-coated glass slides (Muto Purechemicals Co., Japan). After deparaffinization, endogenous peroxidase was blocked by incubation in 3% H_2O_2 for 5 min. We applied six different pretreatment protocols as follows: (1) 98% formic acid for 5 min (designated as FA); (2) hydrated autoclaving at 121°C, 2 atmosphere (atm) for 20 min (with Tomy high-pressure steam sterilizer KS-323. Japan) in distilled water (121DWHA); (3) 121DWHA and 98% formic acid for 5 min (121DWHA/FA); (4) 121DWHA and proteinase K (0.4 mg/ml, Dako, USA) treatment for 1 min (121DWHA/PK); (5) hydrated autoclaving at 135°C, 3 atm for 20 min in distilled water (135DWHA); (6) 135DWHA and 98% formic acid for 5 min (135DWHA/FA). After applying each pretreatment, tissue sections were incubated with 10% goat or horse normal serum (Nichirei, Japan) for 30 min. In this study, we used the avidin-biotin complex methods (ABC kit; Vector Lab., USA) and the horseradish peroxidase-labeled polymer methods (Envision+ kit; Dako). Sections were exposed to primary antibodies for overnight at 4°C or 1 h at room temperature for ABC kit or Envision+ kit, respectively. As negative controls, the sections were exposed for each primary antibody without any pretreatments. The following steps were performed with second antibodies and others according to the each manufacture's instructions. The signals were detected using diaminobenzidine (Simple stain DAB; Nichirei, Japan). Sections were counterstained with Mayer's hematoxylin.

The characteristics of the nine primary antibodies used in this study are summarized in Table 1. For sections prepared from the tissue blocks immersed in 15% formalin for 6 months, we tested the 121DWHA and 135DWHA methods using B103 and 43C5 antibodies.

Table 1 Characteristics of the nine antibodies used in this study (*L* linear epitope, *DC* discontinuous epitope, *mAb* monoclonal antibody, *pAb* polyclonal antibody)

Antibodies	Epitope		Clonality	Dilution	Immunogen	Source
	Position	L/DC				
132	119–127	L	mAb	1:200	Mouse recPrP	Horiuchi
149	147–153	L	mAb	1:500	Mouse recPrP	Horiuchi
43C5	163–169	L	mAb	1:10000	Mouse recPrP	Horiuchi
B103	103–121	L	pAb	1:1000	Cow recPrP	Horiuchi
6H4	155–163	L	mAb	1:500	Cow recPrP	Prionics (Zürich, Switzerland)
72	89–231(143–151)	DC	mAb	1:500	Mouse recPrP	Horiuchi
44B1	155–231	DC	mAb	1:200	Mouse recPrP	Horiuchi
44B2	155–231	DC	mAb	1:200	Mouse recPrP	Horiuchi
T2	Unknown	DC	mAb	1:500	Mouse recPrP	Tagawa

Morphometry

Serial sections from BSE-affected samples were pretreated with 121DWHA, 121DWHA/FA, 121DWHA/PK, 135DWHA, and 135DWHA/FA methods, and immunostained with four antibodies (B103, 43C5, 44B1, and 6H4), respectively. Each of the pretreatment conditions were evaluated on the selected five areas (total μm^2). The Lumina Vision computer analysis system (Mitani Corp., Tokyo, Japan) was used to measure the positive area of PrP immunostaining. The brown-colored chromogen precipitate was selected, digitized images of these areas, and the digital pixels converted into the density area (μm^2) on the software. The highest density measurement was set to 100% and relative density (RD) of immunostaining by the other pretreatments in the same area was calculated.

Results

Histopathology

In the mouse, neuropil vacuolation associated with astrogliosis and microglial proliferation was observed throughout all areas of the brain. Amyloid plaque structures were also seen, which were often observed in contact with the capillary vessels.

In the obex region of scrapie-infected sheep, neuropil vacuolation and single or multiple intracytoplasmic vacuoles were particularly found in the dorsal motor nucleus of vagus nerve (DMNV), gracile nucleus, nucleus ambiguus and reticular formation [22]. The hypoglossal nucleus, olivary nucleus and nucleus of solitary tract (NST) were only mildly affected. In addition, spongiform neuropil lesions were seen in the periphery of the dorsal column of spinal cord and the vertebral column.

In BSE cases, because of the subclinical case, extremely mild spongiform lesions were observed only in the DMNV, and periphery of the reticular formation [24].

Immunohistochemistry

Immunohistochemical examination revealed that no PrP depositions were observed in the sections from the affected animals without pretreatment and from the control animals with and without pretreatment.

PrP^{Sc} immunostaining yielded characteristic patterns in each animals affected with prion disease [21]. The following immunostaining patterns were observed: (1) fine particulate deposition; (2) coarse particulate deposition; (3) perineuronal deposition; (4) glial type deposition; (5) perivascular or perivacuolar deposition; (6) plaque or plaque-like deposition.

In scrapie-infected mice, PrP^{Sc} deposits were observed diffusely in cortex, thalamus, and hippocampus. Perivascular, perivacuolar PrP^{Sc} deposits and plaque or plaque-like structures in thalamus were also seen.

The PrP^{Sc} deposits in scrapie-affected sheep were most intense in the DMNV. The hypoglossal nucleus also showed deposits, but the staining was sparse. Glial, coarse particulate, perineuronal, perivascular and perivacuolar depositions were found in the reticular formation.

In BSE cases, the intense positive reactions of PrP^{Sc} were observed in the DMNV, NST and periphery of the reticular formation, which showed fine, perineuronal and perivacuolar patterns. Fine or coarse particulate depositions were seen in olivary nucleus. The hypoglossal nucleus also showed positive reactions, but with a low intensity of immunostaining.

Comparison of pretreatment methods

Microscopic examinations for each pretreatment and antibody are summarized in Table 2. All antibodies used in this study reacted with PrP^{Sc} of all animals under some

pretreatments.

Table 2 Results of the immunoreactivity for the antibodies under pretreatment methods [*FA* 96% formic acid for 5 min, *121DWHA* hydrated autoclaving at 121°C, 2 atmosphere (atm) for 20 min in distilled water, *121DWHA/FA* 121DWHA and 96% formic acid for 5 min, *121DWHA/PK* 121DWHA and proteinase K treatment for 1 min, *135DWHA* hydrated autoclaving at 135°C, 3 atm for 20 min in distilled water, *135DWHA/FA* 135DWHA and 98% formic acid for 5 min, *M* scrapie-affected mouse, *C* BSE-affected cow, *S* scrapie-affected sheep, *P* plaque type, *D* diffuse type, *3+* strongly positive signal, *2+* moderately positive signal, *+* faint positive signal, *-* negative]

Antibodies	Tissue souce	Pretreatment					
		FA	121DWHA	121DWHA/FA	121DWHA/PK	135DWHA	135DWHA/FA
132	M/P	-	2+	2+	+	2+	2+
	M/D	-	+	2+	-	+	2+
	C	-	-	+	-	3+	3+
	S	-	-	2+	-	2+	3+
149	M/P	2+	+	2+	2+	3+	2+
	M/D	+	+	2+	+	3+	+
	C	-	-	2+	-	+	3+
	S	-	+	2+	2+	2+	3+
43C5	M/P	+	2+	2+	2+	3+	3+
	M/D	-	2+	2+	2+	2+	2+
	C	-	2+	2+	2+	2+	3+
	S	-	2+	2+	2+	3+	3+
B103	M/P	-	+	2+	2+	3+	3+
	M/D	-	+	2+	2+	3+	3+
	C	-	+	2+	2+	3+	3+
	S	-	+	2+	2+	3+	3+
6H4	M/D	-	+	2+	+	-	-
	M/P	-	+	2+	-	-	-
	C	-	+	2+	-	-	-
	S	-	+	2+	-	-	-
72	M/P	2+	+	3+	-	-	2+
	M/D	-	-	+	-	-	-
	C	+	-	2+	+	-	-
	S	-	+	2+	-	-	-
44B1	M/P	+	+	2+	-	+	2+
	M/D	-	-	2+	-	-	2+
	C	+	+	2+	-	-	+
	S	-	-	2+	-	-	+
44B2	M/P	+	+	3+	-	-	2+
	M/D	-	-	2+	-	-	+
	C	-	-	2+	-	-	-
	S	-	-	2+	-	-	-
T2	M/P	2+	+	3+	-	-	+
	M/D	-	-	2+	-	-	-
	C	-	-	2+	-	-	+
	S	-	-	2+	-	-	-

Single FA pretreatment gave very weak or no reactions to all antibodies; however, mouse amyloid plaques were positive to some antibodies (mAbs 149, 43C5, 72, 44B1, 44B2, and T2). Among 121DWHA, and a combination of 121DWHA with FA (121DWHA/FA) or PK (121DWHA/PK) pretreatments, 121DWHA/FA was most effective with most antibodies, but 121DWHA/PK was more or equally effective compared with 121DWHA/FA using mAb 43C5 and pAb B103. Considering the sensitivity to 135DWHA and 135DWHA/FA pretreatments, the antibodies used in this study have been divided into two types, one which showed the increase in reactivity, and the other showing a significant reduction or a loss of reactivity. mAbs 132, 149, 43C5 and pAb B103, which reacted with the linear epitope, are classified to the former group (Fig. 1a–d), while mAbs 72, 44B1, 44B2 and T2 recognizing the discontinuous epitope are referred to the latter group (Fig. 2a–d). mAb 6H4 against cow recombinant PrP stained bovine, ovine and murine PrP^{Sc} with 121DWHA/FA pretreatment, but other pretreatments showed no positive reactions for any animal PrP^{Sc} except for the murine plaque type of PrP^{Sc} with 121DWHA, 121DWHA/FA and 121DWHA/PK pretreatments.

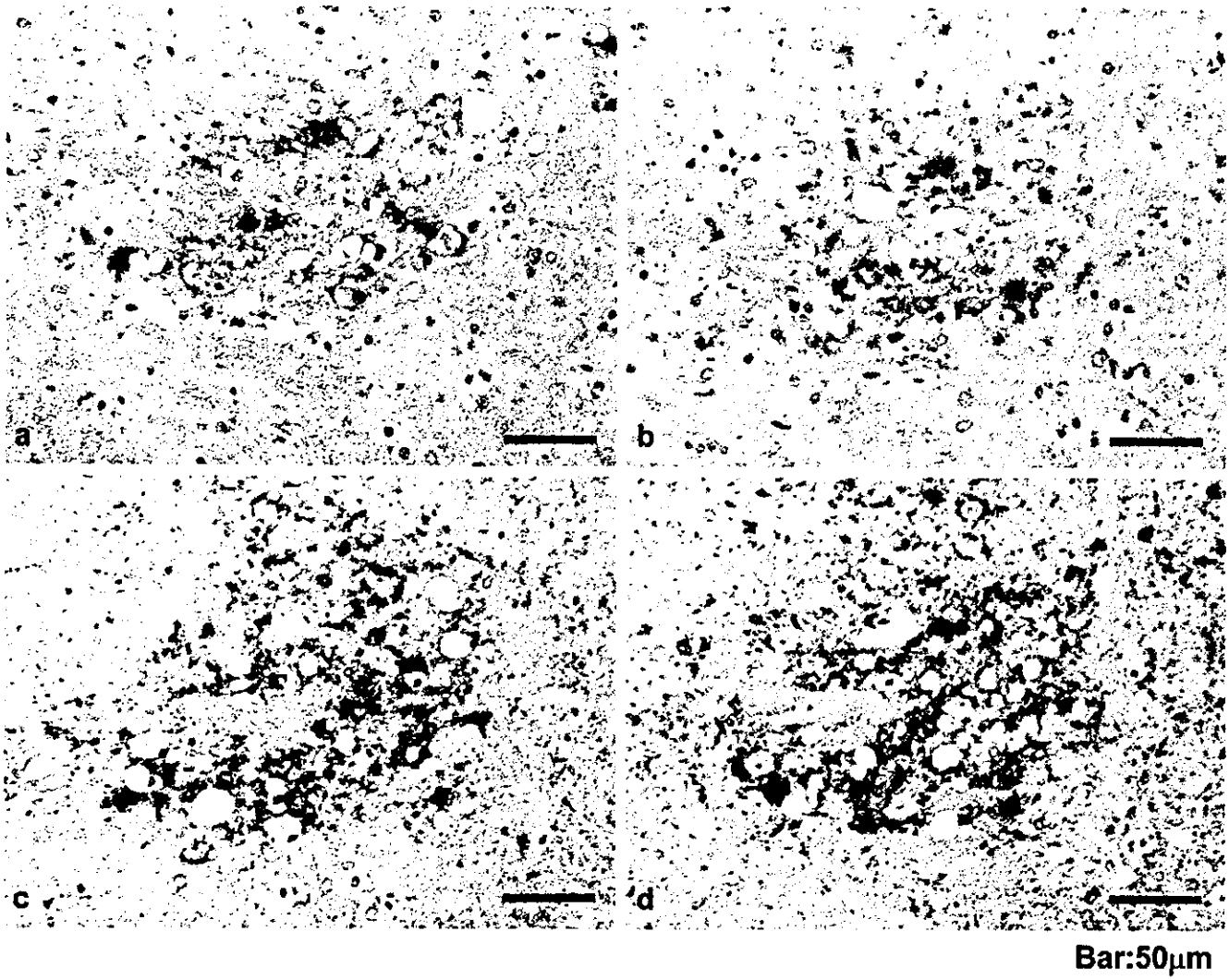

Fig. 1 Immunohistochemistry of the PrP with mAb 43C5 in the thalamus of scrapie-affected mouse; **a** 121DWHA, **b** 121DWHA/FA, **c** 135DWHA and **d** 135DWHA/FA methods. The immunodensity is considerably greater using the 135DWHA and 135DWHA/FA methods [*PrP* prion protein, *121DWHA* hydrated autoclaving at 121°C, 2 atmosphere (atm) for 20 min in distilled water, *121DWHA/FA* 121DWHA and 96% formic acid for 5 min, *135DWHA* hydrated autoclaving at 135°C, 3 atm for 20 min in distilled water, *135DWHA/FA* 135DWHA and 98% formic acid for 5 min]. *Bars* **a**–**d** 50 μm

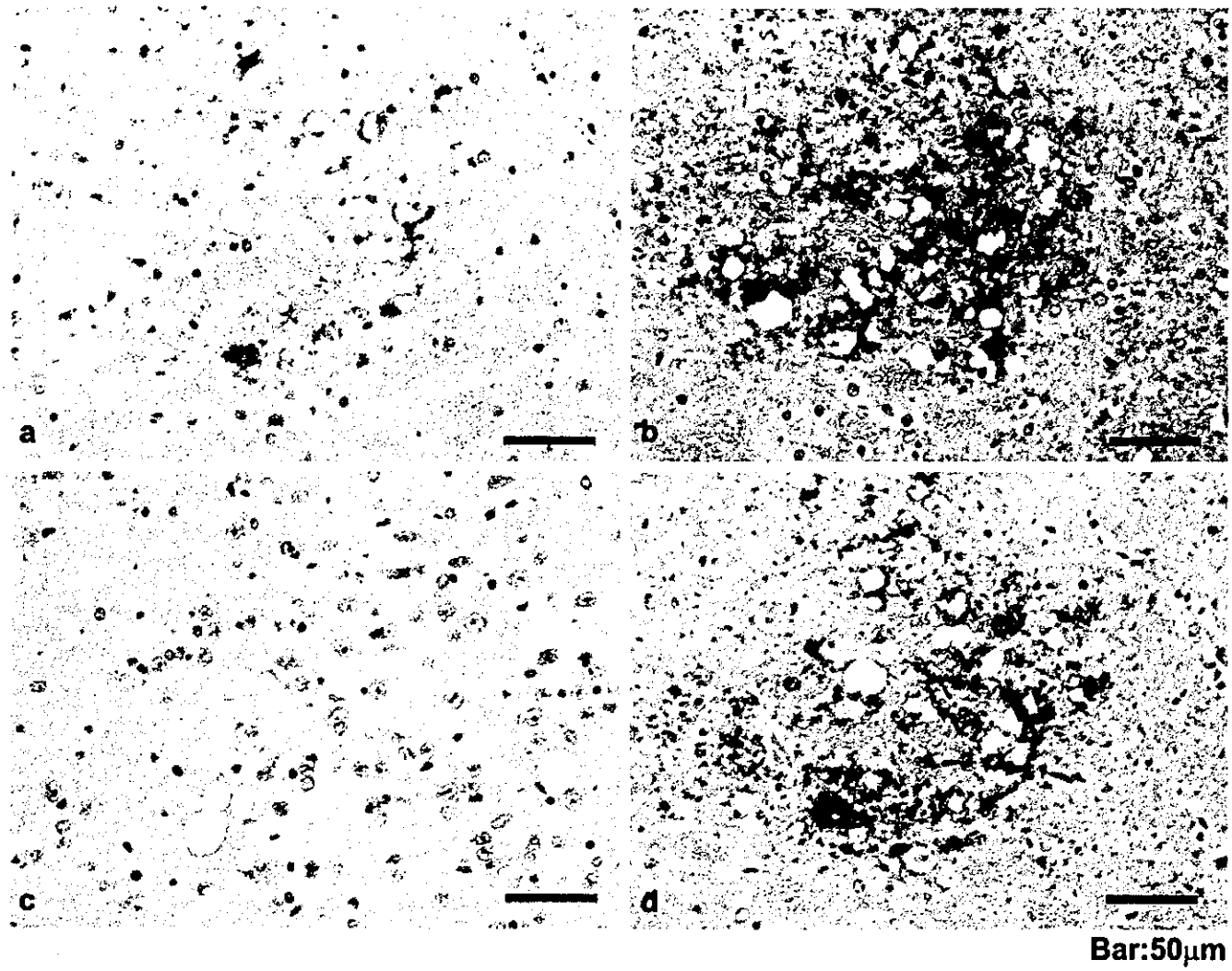

Fig. 2 Immunohistochemistry of the PrP with mAb 44B1 in the thalamus of scrapie-affected mouse; **a** 121DWHA, **b** 121DWHA/FA, **c** 135DWHA and **d** 135DWHA/FA methods. The 121DWHA/FA method is the most effective for enhancing the PrP and only faint reactivity is observed with the 121DWHA method. Although 135DWHA/FA method enhances the PrP, no reactive deposits are observed using the 135DWHA method. *Bars* a–d 50 μm

Effects on the sections from the tissues immersed in formalin for a long period

With 121DWHA and 135DWHA pretreatment, both B103 and 43C5 antibodies gave positive reactions in almost the same areas for sections of scrapie-affected sheep that had been immersed in formalin for 6 months. However, the sections treated by the 135DWHA method yielded an intense signal and widespread staining, while the detectable antigens in 121DWHA pretreatment were limited and showed low intensity (Fig. 3a, b).

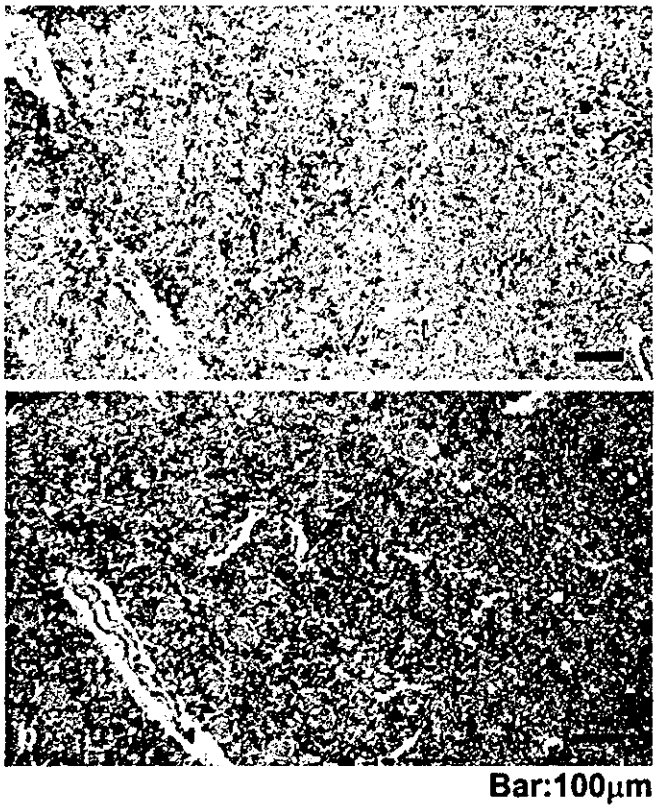

Fig. 3 Immunohistochemistry of the PrP with pAb B103 in the sections of scrapie-affected sheep from the sample immersed in formalin for 6 months; **a** 121DWHA and **b** 135DWHA methods. *Bars* **a**, **b** 500 μm

Morphometry

The comparison of RD in each pretreatment method on BSE sections is shown in Fig. 4. This digital morphometry was in good agreement with the observations throughout. Although 135DWHA or 135DWHA/FA methods increased the density with mAb 43C5 and pAb B103, the effect was stronger with the former (Fig. 4a, b). Using mAbs 44B1 and 6H4, the 121DWHA/FA protocol was appropriate for antigen retrieval and the 135DWHA or 135DWHA/FA method were not effective (Fig. 4c, d).

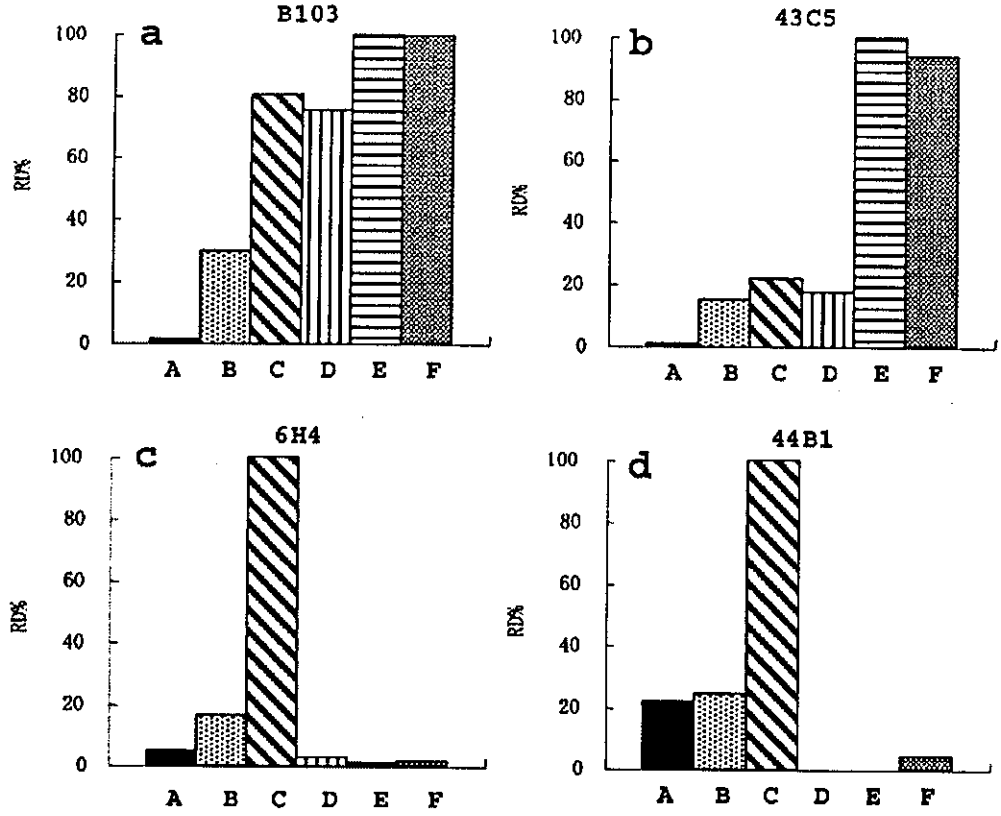

Fig. 4 Comparison of relative density (*RD%*) using each pretreatment method on BSE sections for different antibodies; **a** pAb B103, **b** mAb 43C5, **c** mAb 6H4, and **d** mAb 44B1. mAb 44B1 recognizes discontinuous epitope, and others recognize linear epitope. The effect of FA, 121DWHA, 121DWHA/FA, 121DWHA/PK, 135DWHA and 135DWHA/FA is displayed as *bar A*, B, *C*, *D*, *E* and *F*, respectively. **a** FA displays 1 RD%. 121DWHA (29 RD%) does not lead to a significant increase. 121DWHA/FA and 121DWHA/PK show a density of 81 and 75 RD%, respectively. Immunodensity is further enhanced by 135DWHA (100 RD%) and 135DWHA/FA (100 RD%). **b** FA displays 1 RD%. 121DWHA, 121DWHA/FA and 121DWHA/PK show 15, 22 and 18 RD%, respectively. 135DWHA and 135DWHA/FA result in 100 and 94 RD%, showing a significant increase. **c** FA (5 RD%), 121DWHA (17 RD%), 121DWHA/PK (3 RD%), 135DWHA (1 RD%) and 135DWHA/FA (2 RD%) do not lead to a significant increase in immunodensity. 121DWHA/FA (100 RD%) shows the highest increase. **d** FA shows 22 RD% and 121DWHA 25 RD%. Imunodensity is not enhanced by 121DWHA/PK and 135DWHA. 135DWHA/FA displays 4 RD%. The best result was obtained by 121DWHA/FA (100 RD%) (*FA* 96% formic acid for 5 min, *121DWHA/PK* 121DWHA and proteinase K treatment for 1 min)

Discussion

In immunohistochemistry for the prion diseases, several pretreatment methods to enhance the immunoreactivity of human and animal PrP^{Sc} on the tissue sections have been reported. The method of 121°C hydrated autoclaving pretreatment or the combination method of 121°C hydrated autoclaving with a certain chemical reagent (formic acid or proteinase K, etc) are now widely used [5, 13]. The precise mechanisms by which pretreatments enhance the PrP^{Sc} immunoreactivity are still unknown. However, the effect of these chemical treatments is considered to make amyloid fibril proteins denature, breaking down the structure of amyloid fibrils, and exposing the buried epitopes [4]. In formic acid pretreatment, microwave irradiation is thought to enable for formic acid penetration in tissue, and to expose the epitope and react with the antigen more efficiently [7]. In addition, it is speculated that hydrolytic autoclaving contributes to alter the primary structures of PrP in situ [11].

We describe a new hydrated autoclaving method, termed the 135DWHA method, to enhance the immunoreactivity of the PrP^{Sc}, and have compared this with the previously reported methods. Generally, the 135DWHA or 135DWHA/FA methods for the antibodies reacting with linear epitope showed a higher sensitivity than 121DWHA, 121DWHA/FA, or 121DWHA/PK methods, except for antibody 6H4. Although prolonged exposure of brain material to aldehyde fixatives usually dramatically decreases the antigenicity of PrP^{Sc} [17], this newly enhancing method was more effective for the long-term fixation samples compared with other methods. On the other hand, our simple modification could not enhance immunoreactivity for the prion antigen for antibodies recognizing discontinuous or conformational epitopes.

For immunohistochemical antigen-retrieval techniques, hypotheses such as breaking cross-linking [16], protein denaturation or modification-re-modification [3] have been proposed, and were thought to have an advantage on the basis of observation or support from several studies [18, 22, 23]. In particular, the later theory is based on heat- or chemical-induced modification of the three-dimensional structure of "formalinized" protein, restoring the condition of a formalin-modified protein structure back towards its original structure on the paraffin-embedding tissue sections. Because immunohistochemistry without pretreatment did not give any positive reactions using the pAb B103 and 44B1 in the frozen sections (data not shown), there are some differences between this theory and our model. However, it seemed probable that epitopes hidden by the aggregation of PrPs are exposed on the surface, or that conformational binding sites formed by the other protein molecules are disrupted due to conformational changes induced by the hydrating autoclave methods on the formalin-fixed paraffin sections, assuming that the principle of the antigen-retrieval methods is to lead to a re-naturation or partial restoration of the protein structure with re-establishment of the three-dimensional to something approaching its native condition [22, 23].

Antibody, especially that reacting on the discontinuous epitope, recognizes specific epitopes localized in a spatial configuration within the protein molecule. mAb 15B3 recognizes the discontinuous epitope in the pathological PrP isoform, and a single continuous 15B3 binding site was speculated to be formed either by aggregation of two or several PrP molecules, or by structural rearrangement of a single PrP molecule, or by a combination thereof [12]. The exact mechanisms causing the differences between 135DWHA and 121DWHA methods in the antibody's recognition of the conformational epitope are still unknown. However, these can be surmised as follows: some aggregate proteins or molecules may be loosely arranged and antigenic determinants come to lie on the surface during formic acid or 121°C, 2 atm autoclaving pretreatment; furthermore, elevation of the temperature and atmosphere may cause further changes of certain stereoscopic structures or components of PrP molecules, causing a loss of its conformational epitope. Additional formic acid treatment also causes a slight change, helping in the demasking of the conformational epitope.

Further studies on prion antigen-retrieval techniques, including establishing an exact correlation of these mechanisms and the antibody epitope, may shed new light in the pathology of the prion diseases.

Acknowledgements This work was supported by a Grant-in-Aid for Exploratory Research from the Ministry of Education, Culture, Sports, Science and Technology of Japan (grant 14656118) and a Grant from the Ministry of Health, Labor and Welfare of Japan (grant 14240101).

References

1. Bell JE, Gentleman SM, Ironside JW, McCardle L, Lantos PL, Fergusson J, Luthert P, McQuaid S, Allen IV (1997) Prion protein immunocytochemistry-UK five centre consensus report. Neuropathol Appl Neurobiol 23:26–35
CrossRef | ChemPort | PubMed

2. Bodemer W (1999) The use of monoclonal antibodies in human prion disease. Naturwissenschaften 86:212–220
SpringerLink | ChemPort | PubMed

3. Cattoretti G, Pileri S, Parravicini C, Becker MHG, Poggi S, Bifulco C, Key G, D'Amato L, Sabattini E, Feudale E, Reynolds F, Gerdes J, Rilke F (1993) Antigen unmasking on formalin-fixed, paraffin-embedded tissue sections. J pathol 171:83–98
ChemPort | PubMed

4. Doi-Yi R, Kitamoto T, Tateishi J (1991) Immunoreactivity of cerebral amyloidosis is enhanced by protein denaturation treatments. Acta Neuropathol 82:260–265
SpringerLink | ChemPort | PubMed

5. Everbroeck BV, Pals P, Martin JJ, Cras P (1999) Antigen retrieval in prion protein immunohistochemistry. J Histochem Cytochem 47:1465–1467
PubMed

6. Haritani M, Spencer YI, Wells GAH (1994) Hydrated autoclave pretreatment enhancement of prion protein immunoreactivity in formalin-fixed bovine spongiform encephalopathy-affected brain. Acta Neuropathol 87:86–90
ChemPort | PubMed

7. Hashimoto K, Mannen T, Nukina N (1992) Immunohistochemical study of kuru plaques using antibodies against synthetic prion protein peptides. Acta Neuropathol 83:613–617
SpringerLink | ChemPort | PubMed

8. Hayward PAR, Bell JE, Ironside JW (1994) Prion protein immunocytochemistry: reliable protocols for the investigation of Creutzfeldt-Jacob disease. Neuropathol Appl Neurobiol 20:375–383
ChemPort | PubMed

9. Hegyi I, Hainfellner JA, Flicker H, Ironside J, Hauw JJ, Tateishi J, Haltia M, Bugiani O, Aguzzi A, Budka H (1997) Prion protein immunocytochemistry: reliable staining protocol, immunomorphology, and diagnostic pitfalls. Clin Neuropathol 16:262–263

10. Kitamoto T, Ogomori K, Tateishi J, Prusiner SB (1987) Formic acid pretreatment enhances immunostaining of cerebral and systemic amyloids. Lab Invest 57:230–236
ChemPort | PubMed

11. Kitamoto T, Shin RW, Doh-ura K, Tomokane N, Miyazono M, Muramoto T, Tateishi J (1992) Abnormal isform of prion proteins accumulates in the synaptic structures of the central nervous system in patients with Creutzfeldt-Jakob disease. Am J Pathol 140:1285–1294
ChemPort | PubMed

12. Korth C, Stierli B, Streit P, Moser M, Schaller O, Fischer R, Schulz-Schaeffer W, Kretzschmar H, Raeber A, Braun U, Ehrensperger F, Hornemann S, Glockshuber R, Riek R, Billeter M, Wüthrich K, Oesch B (1997) Prion (PrP^{Sc})-specific epitope defined by a monoclonal antibody. Nature 390:74–77
CrossRef | ChemPort | PubMed

13. Kovács GG, Head MW, Hegyi I, Bunn TJ, Flicker H, Hainfellner JA, McCardle L, László L, Jarius C, Ironside JW, Budka H (2002) Immunohistochemistry for the prion protein: comparison of different monoclonal antibodies in human prion disease subtypes. Brain Pathol 12:1–11

14. Liberski PP, Yanagihara R, Brown P, Kordek R, Kloszewska I, Bratosiewicz J, Gajdusek DC (1996) Microwave treatment enhances the immunostaining of amyloid deposits in both the transmissible and non-transmissible brain amyloidoses. Neurodegeneration 5:95–99
CrossRef | ChemPort | PubMed

15. MacDonald ST, Sutherland K, Ironside JW (1996) A quantitative and qualitative analysis of prion protein immunohistochemical staining in Creutzfeldt-Jacob disease using four anti prion protein antibodies. Neurodegeneration 5:87–94
CrossRef | ChemPort | PubMed

16. Mason JT, O'Leary TJ (1991) Effects of formaldehyde fixation on protein secondary structure: a calorimetric and infrared spectroscopic investigation. J Histochem Cytochem 39:225–229
ChemPort | PubMed

17. McBride PA, Bruce ME, Fraser H (1988) Immunostaining of scrapie cerebral amyloid plaques with antisera raised to scrapie-associated fibrils (SAF). Neuropathol Appl Neurobiol 14:325–336
ChemPort | PubMed

18. Montero C (2003) The antigen-antibody reaction in immunohistochemistry. J Histochem Cytochem 51:1–4

19. Privat N, Sazdovitch V, Seilhean D, Laplanche JL, Hauw JJ (2000) PrP immunohistochemistry: different protocols, including a procedure for long formalin fixation, and a proposed schematic classification for deposits in sporadic Creutzfeldt-Jacob disease. Microsc Res Tech 50:26–31
crossref | ChemPort | PubMed

20. Prusiner SB (1998) Prions. Proc Natl Acad Sci USA 95:13363–13383
crossref | ChemPort | PubMed

21. Ryder SJ, Spencer YI, Bellerby PJ, March SA (2001) Immunohistochemical detection of PrP in the medulla oblongata of sheep: the spectrum of staining in normal and scrapie-affected sheep. Vet Rec 148:7–13
ChemPort | PubMed

22. Shi S-R, Cote RJ, Taylor CR (1997) Antigen retrieval immunohistochemistry: past, present, and future. J Histochem Cytochem 45:327–343
ChemPort | PubMed

23. Shi S-R, Cote RJ, Taylor CR (2001) Antigen retrieval techniques: current perspectives. J Histochem Cytochem 49:931–937
ChemPort | PubMed

24. Wells GAH, Wilesmith JW, McGill IS (1992) Bovine spongiform encephalopathy. Brain Pathol 1:69–78

Available online at www.sciencedirect.com
SCIENCE DIRECT®
Biochemical and Biophysical Research Communications 313 (2004) 850–855
BBRC
www.elsevier.com/locate/ybbrc

Prion protein suppresses perturbation of cellular copper homeostasis under oxidative conditions

Akikazu Sakudo,[a] Deug-chan Lee,[a] Etsuro Yoshimura,[b] Seiji Nagasaka,[b] Kayako Nitta,[a] Keiichi Saeki,[a] Yoshitsugu Matsumoto,[a] Sylvain Lehmann,[c] Shigeyoshi Itohara,[d] Suehiro Sakaguchi,[e] and Takashi Onodera[a,*]

[a] *Department of Molecular Immunology, School of Agricultural and Life Sciences, University of Tokyo, Bunkyo-ku, Tokyo 113-8657, Japan*
[b] *Department of Applied Biological Chemistry, School of Agricultural and Life Sciences, University of Tokyo, Bunkyo-ku, Tokyo 113-8657, Japan*
[c] *Institut de Genetique Humaine, CNRS U.P.R. 1142, 141, rue de la Cardonille, Montpellier 34396, France*
[d] *Laboratory for Behavioral Genetics, Brain Science Institute, RIKEN, Wako, Saitama 351-0198, Japan*
[e] *Departments of Molecular Microbiology and Immunology, Nagasaki University Graduate School of Biomedical Sciences, Sakamoto, Nagasaki 852-8523, Japan*

Received 27 November 2003

Abstract

Prion protein (PrP) binds copper and exhibits superoxide dismutase-like activity, while the roles of PrP in copper homeostasis remain controversial. Using Zeeman graphite furnace atomic absorption spectroscopy, we quantified copper levels in immortalized PrP gene (*Prnp*)-deficient neuronal cells transfected with *Prnp* and/or *Prnd*, which encodes PrP-like protein (PrPLP/Dpl), in the presence or absence of oxidative stress induced by serum deprivation. In the presence of serum, copper levels were not significantly affected by the expression of PrP and/or PrPLP/Dpl, whereas serum deprivation induced a decrease in copper levels that was inhibited by PrP but not by PrPLP/Dpl. The inhibitory effect of PrP on the decrease of copper levels was prevented by overexpression of PrPLP/Dpl. These findings indicate that PrP specifically stabilizes copper homeostasis, which is perturbed under oxidative conditions, while PrPLP/Dpl overexpression prevents PrP function in copper homeostasis, suggesting an interaction of PrP and PrPLP/Dpl and distinct functions between PrP and PrPLP/Dpl on metal homeostasis. Taken together, these results strongly suggest that PrP, in addition to its antioxidant properties, plays a role in stabilizing cellular copper homeostasis under oxidative conditions.

Keywords: Prion protein; PrPLP/Dpl; PrP-deficient cell line; Copper; Manganese

The function of the cellular isoform of prion protein (PrP^C) remains unclear. Several lines of recent evidence suggest that PrP^C binds copper and has antioxidative activity, especially contributing to superoxide dismutase (SOD) activity [1–6]. Although manganese can substitute for copper, it induces conformational changes and a loss of SOD activity [7]. Furthermore, the implication of metal or oxidative stress metabolism in the pathogenesis of prion diseases has been reported. Brain from prion-infected animals shows a decrease in copper level with a concomitant increase in manganese level [8]. A reduction in copper level and an elevation in manganese level were demonstrated for affinity-purified prion protein (PrP) from prion-infected animals [9]. Moreover, brains in scrapie-infected animals show increased levels of oxidative stress markers [8,10].

Some lines of PrP gene (*Prnp*)-knockout $Prnp^{-/-}$ mice (ZrchII, Ngsk, Rcm0, and Rikn) expressing PrP-like protein PrPLP/Dpl [11,12], which is encoded by *Prnd*, exhibit a late-onset ataxia that can be rescued by crossing the mice with those overexpressing wild-type PrP [13,14], suggesting that PrP^C functionally interacts with PrPLP/Dpl. The predicted protein of PrPLP/Dpl has ~25% identity with the carboxy-terminal two-thirds of PrP [11]. These proteins revealed a similar three-dimensional structure in a nuclear magnetic resonance (NMR) study [15]. Unlike PrP^C, PrPLP/Dpl lacks the

* Corresponding author. Fax. +81-3-5841-8020.
E-mail address: aonoder@mail.ecc.u-tokyo.ac.jp (T. Onodera).

0006-291X/$ - see front matter © 2003 Elsevier Inc. All rights reserved.
doi:10.1016/j.bbrc.2003.12.020

N-terminal octa-peptide repeat region of PrP^C to which copper ions are bound [11]. Conflicting results have so far been reported for the capability of PrPLP/Dpl to bind copper ions. One recent report has shown that this protein binds to copper [16], while another does not [17]. Moreover, PrPLP/Dpl expression correlates to the levels of oxidative stress markers in the brains of PrP-knockout mice, suggesting PrPLP/Dpl exacerbates oxidative stress [18]. Therefore, the expression of both proteins can have an important role in metal homeostasis and oxidative stress metabolism.

Recent studies have demonstrated a decrease in copper content in the brain of ZrchI PrP-knockout mice compared to those of wild-type mice [2], whereas other studies have provided inconsistent results [19]. Moreover, the regulation of copper concentration by PrP^C may not be a cell-autonomous mechanism but rather reflect a systemic process of heterogeneous cell population in the brain. Therefore, the cell-autonomous role of PrP^C in metal homeostasis was estimated by investigating the metal levels in the presence or absence of PrP^C in *Prnp*$^{-/-}$cells. Additionally, the role of PrPLP/Dpl in metal homeostasis is unknown. We therefore investigated whether PrP^C and PrPLP/Dpl expression could affect metal homeostasis in vitro and in vivo.

Materials and methods

Cell cultures and animals. A murine PrP-deficient cell line (HpL3-4) [20] and the transfectants (HpL3-4-PrPNo3 [21], HpL3-4-EM, HpL3-4-PrP, HpL3-4-Dpl, and HpL3-4-PrPDpl) were maintained in Dulbecco's modified Eagle's medium (DMEM) (Sigma, St. Louis, MO) supplemented with 10% fetal calf serum (FCS) at 37 °C in a humidified 5% CO_2 incubator. Serum deprivation was performed as previously described [21]. Male Rikn *Prnp*$^{-/-}$ mice (ectopically expressing PrPLP/Dpl) [22], male FVB/*Prnp*$^{-/-}$ (ZrchI) mice (not ectopically expressing PrPLP/Dpl) (kindly provided by Dr. Stanley B. Prusiner), and male C57BL/6CrSlc (*Prnp*$^{+/+}$) mice (Japan SLC, Hamamatsu, Japan) were analyzed at 10 weeks of age. All mice were housed according to standard animal care protocols in accordance with guidelines of the University of Tokyo and fed standard laboratory chow (CLEA Rodent Diet CE-2; CLEA Japan, Inc., Tokyo, Japan) and tap water ad libitum. The number of animals was kept to a minimum, and the animals were sacrificed in accordance with guidelines of the University of Tokyo before the collection of their brains.

Plasmid construction and gene transfer. The open-reading frame (ORF) of PrPLP/Dpl cDNA was amplified by polymerase chain reaction (PCR) using DPL-KOZAK-SF (5′-GCGTCGACC[GCCACCATGA]AGAACCGGCTGGGTACATGG-3′). [The *Sal*I linker is underlined and the Kozak consensus sequence (GCCACCATGG) is boxed [23]] and DPL-STOP-SR (5′-CTCGTCGACCTCTGTGGCTGCCAGCTTCATTGA-3′) primer, subcloned into pT7Blue vector, and cloned into pIRES-EGFP vector (Clontech, Palo Alto, CA) in the sense orientation to the cytomegalovirus promoter. The Dpl-EGFP fragment was cut out and inserted into the multi-cloning site of pMSCVhyg vector (Clontech). The resulting constructs were pMSCVhyg-EGFP and pMSCVhyg-EGFP-Dpl. In these vectors, the viral long terminal repeat drives expression of the hygromycin resistance gene whereas the murine stem cell virus (MSCV) promoter drives transgene expression. The pMSCV constructs were transiently transfected into the packaging cell line PT67 by the lipofectamine-mediated method (Gibco/BRL, Gaithersburg, MD). Viral supernatants were harvested and used to transduce HpL3-4-PrPNo3 cells or HpL3-4 cells transfected with pMSCVpuro. Selection was performed for more than 10 days in a complete medium containing 400 μg/ml hygromycin (WAKO, Osaka, Japan).

Antibodies. Antibodies DDC39 [24] and 6H4 (Prionics, Zürich, Switzerland) [25] were, respectively, used for the detection of mouse PrPLP/Dpl and mouse PrP^C.

Determination of metal concentration. To minimize metal contamination of samples, all vessels and scrapers were immersed in 0.1 M nitric acid overnight and washed with deionized water. Brains were dissected from male adult (10 week old) mice. Cells were collected by scraper and washed four times with phosphate-buffered saline (PBS). Tissue and cell samples were frozen at −80 °C prior to use. The sample was taken and dried at 105 °C for 4 h in a 10-ml polytetrafluoroethylene beaker to obtain the dry weight. The sample and 0.5 ml of concentrated HNO_3 were heated separately from room temperature to 150 °C for over 1 h and then kept at 150 °C for 6 h to promote vapor phase digestion of HNO_3 in a 50-ml polytetrafluoroethylene digestion vessel with a stainless steel jacket [26]. After cooling to room temperature, the container was diluted to 2 ml with 0.1 M HNO_3. The concentrations of Cu and Mn were determined by graphite furnace atomic absorption spectroscopy (GF-AAS) with polarized Zeeman-effect background correction (Hitachi Z-9000 atomic absorption spectrophotometer, Japan). Analysis lines used were 324.8 and 279.5 nm for Cu and Mn, respectively. The following thermal treatment program was used: drying from 80 to 120 °C for 30 s, ashing from 300 to 600 °C for 30 s, holding at 600 °C for 10 s, atomization at 2700 °C for 10 s, and cleaning at 3000 °C for 3 s. The argon gas purged at a flow rate of 200 ml/min during the drying and ashing cycles and 30 ml/min during atomization. The signal intensity was calibrated with standard solutions of Cu or Mn. We measured each brain or cell pellet sample in triplicate and the mean value was employed for analysis. The metal values presented are means (μg/g) dry weight. Values represented means ± SE of each group ($N = 4$) of mouse brains or cell pellets analyzed.

Western blot assay. The procedures for protein extraction from brains and cells and subsequent immunoblotting have been described previously [21] with DDC39 anti-PrPLP/Dpl antiserum or 6H4 anti-PrP monoclonal antibody. Equal quantities of protein (60 μg for PrP^C and 60 μg for PrPLP/Dpl) were used for Western blotting.

Statistical analysis. Statistical analysis was performed using the non-repeated measures ANOVA followed by Dunnett's test. Differences where $p < 0.05$ were considered to be statistically significant.

Results and discussion

To investigate whether PrPLP/Dpl plays a role similar to PrP^C in the regulation of copper and manganese homeostasis, copper and manganese concentrations were determined for the HpL3-4 cells transfected with *Prnp* and/or *Prnd*. The expression of PrP^C and PrPLP/Dpl in the stable transfectants was confirmed by Western blot analysis using anti-PrP 6H4 and anti-PrPLP/Dpl DDC39 (Fig. 1A). HpL3-4-PrP cells expressed PrP^C at a level equivalent to that in HpL3-4-PrPDpl cells, while no apparent PrP^C were observed in HpL3-4-EM and HpL3-4-Dpl cells. Although reverse transcription-PCR indicated the presence of PrP-PrPLP/Dpl chimeric mRNA in HpL3-4 cells (D.C. Lee, A. Sakudo, T. Onodera, unpublished results), PrPLP/Dpl protein was under the detectable limit in HpL3-4-EM and HpL3-4-PrP cells by Western blot analysis employing 60 μg of

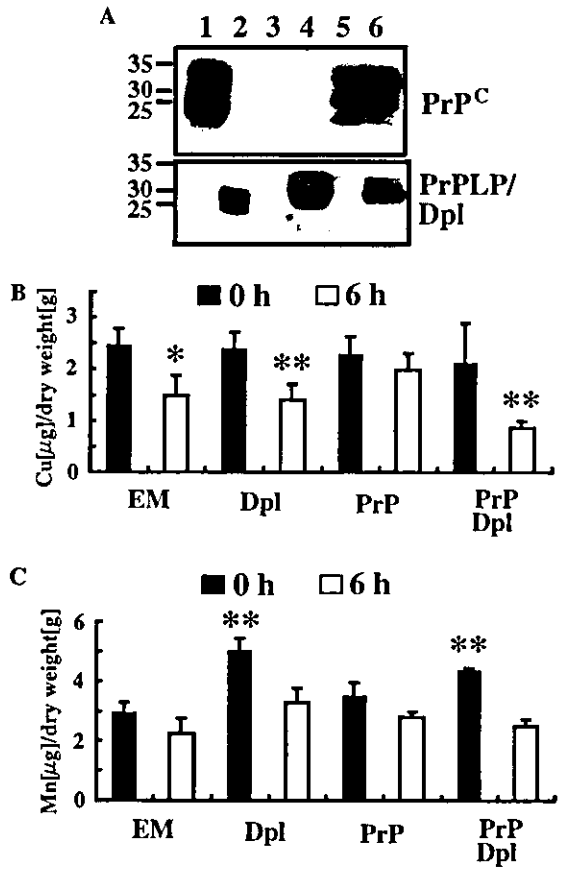

Fig. 1. Cellular copper and manganese content in *Prnp*$^{-/-}$ cells transfected with *Prnp* and/or *Prnd*. Cellular copper and manganese content in *Prnp*$^{-/-}$ cells transfected with *Prnp* and/or *Prnd* cultured in the absence and presence of serum was determined by graphite furnace atomic absorption spectroscopy (GF-AAS) with Zeeman background correction. (A) *Prnp*$^{+/+}$ (WT) brain (lane 1), Rikn *Prnp*$^{-/-}$ brain (lane 2), and HpL3-4 cells transfected with pMSCVpuro + pMSCVhyg-EGFP (EM: HpL3-4-EM; lane 3), pMSCVpuro + pMSCVhyg-EGFP-Dpl (Dpl: HpL3-4-Dpl; lane 4), and pMSCV puro-PrP + pMSCVhyg-EGFP (PrP: HpL3-4-PrP; lane 5) or pMSCV puro-PrP + pMSCVhyg-EGFP-Dpl (PrPDpl: HpL3-4-PrPDpl; lane 6) were separated by sodium dodecyl sulfate (SDS)–polyacrylamide gel electrophoresis (PAGE) and then Western blotted. PrP^{C} or PrPLP/Dpl was detected with 6H4 or DDC39, respectively. (B,C) Cellular copper (B) and manganese (C) content in HpL3-4 cells transfected with *Prnp* and/or *Prnd* and serum-deprived for 0 h (black bars) or 6 h (white bars). Differences where $p < 0.05$ (*) and < 0.01 (**) compared with HpL3-4-EM cells serum-deprived for 0 h were considered statistically significant.

extracted protein (Fig. 1A). However, enhanced levels of PrPLP/Dpl were observed in HpL3-4-Dpl and HpL3-4-PrPDpl cells compared to HpL3-4-EM and HpL3-4-PrP cells. The cellular copper concentration among HpL3-4-EM, HpL3-4-PrP, HpL3-4-Dpl, and HpL3-4-PrPDpl cells was not significantly different in the presence of serum (Fig. 1B). Therefore, the expression of PrP^{C} and PrPLP/Dpl did not influence cellular copper homeostasis in the presence of serum. We examined the changes of cellular copper levels after 6 h of serum deprivation, a period which corresponds to the time required for superoxide generation [21]. The incubation of cells in the absence of serum significantly decreased cellular copper concentration in HpL3-4-EM, HpL3-4-Dpl, and HpL3-4-PrPDpl cells, whereas that in HpL3-4-PrP cells was unchanged (Fig. 1B). These results demonstrated that PrP^{C} prevented a decrease in cellular copper concentration under serum deprivation.

We analyzed the effect of the expression of PrP^{C} and PrPLP/Dpl on cellular manganese concentration using PrP-deficient cells. In the presence of serum, HpL3-4-Dpl and HpL3-4-PrPDpl cells showed manganese concentration significantly higher than HpL3-4-EM and HpL3-4-PrP cells (Fig. 1C), with HpL3-4-PrP cells being not significantly different in manganese content compared with HpL3-4-EM cells (Fig. 1C). The increase in manganese concentration was correlated with the expression level of PrPLP/Dpl (Fig. 1C). Therefore, the cellular concentration of manganese was regulated by PrPLP/Dpl in an expression level-dependent manner but not by PrP^{C} in the presence of serum. However, after incubation in serum-free culture for 6 h, all four transfectants did not show any significant differences in cellular manganese content (Fig. 1C). These results suggest that the expression of PrPLP/Dpl enhanced manganese uptake from serum in an expression level-dependent manner and PrP^{C} did not influence cellular manganese homeostasis.

To further examine whether copper and manganese content is regulated by the expression of PrP and PrPLP/Dpl in vivo, copper and manganese contents in brains of *Prnp*$^{+/+}$, Rikn *Prnp*$^{-/-}$, and FVB/*Prnp*$^{-/-}$ (ZrchI) mice were analyzed. The brain Cu concentration depends on diet and age [27,28]. This may account for some of the contradictory results concerning copper concentrations between wild-type and ZrchI PrP-knockout mice [2,19]. Therefore, in this study to minimize the effect of age and diet on the results in all three mouse lines (*Prnp*$^{+/+}$ mice, Rikn *Prnp*$^{-/-}$, and FVB/*Prnp*$^{-/-}$ (ZrchI)), we used age-matched male mice fed with standard diet (CLEA Rodent Diet CE-2; CLEA Japan, Inc., Tokyo, Japan), in which the metal content was monitored (8.1 ± 0.9 Cu μg/g dry weight, 105.3 ± 6.9 Mn μg/g dry weight). *Prnp*$^{+/+}$ mice expressed PrP^{C} but not PrPLP/Dpl in the brain (Fig. 2A); a Western blot analysis confirmed that brains of Rikn *Prnp*$^{-/-}$ mice showed ectopic PrPLP/Dpl expression without PrP^{C} expression (Fig. 2A), while those of FVB/*Prnp*$^{-/-}$ (ZrchI) mice demonstrated the absence of both proteins (Fig. 2A). Rikn *Prnp*$^{-/-}$ brain demonstrated a significant decrease in copper concentration compared to *Prnp*$^{+/+}$ brain, whereas FVB/*Prnp*$^{-/-}$ (ZrchI) brain showed no significant difference in copper concentration from *Prnp*$^{+/+}$ brain (Fig. 2B). In comparison, although an increased manganese content by PrPLP/Dpl expression was observed at a cellular level (Fig. 1C), brains of Rikn *Prnp*$^{-/-}$ mice ectopically expressing PrPLP/Dpl revealed no difference in manganese content when compared to those of *Prnp*$^{+/+}$ mice (Fig. 2C).

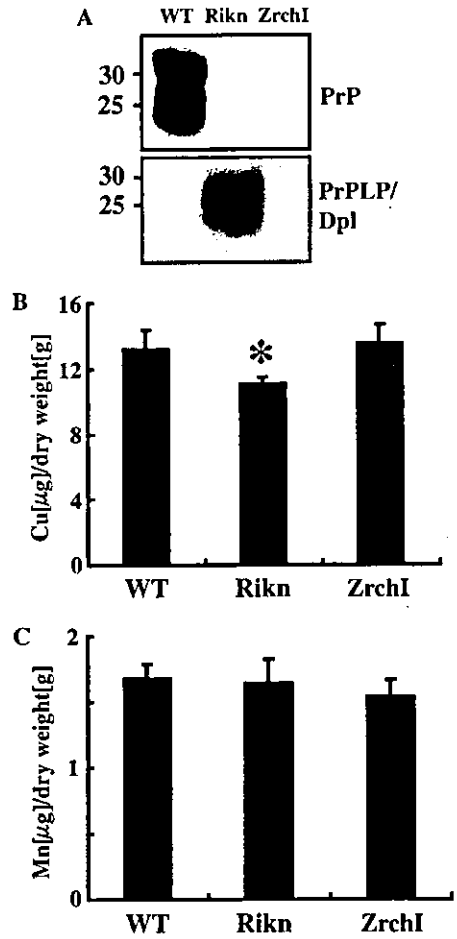

Fig. 2. Effect of PrP^C and PrPLP/Dpl expression on brain metal levels. (A) PrP^C and PrPLP/Dpl expressions in *Prnp*$^{+/+}$ (WT) brain and Rikn *Prnp*$^{-/-}$ and FVB/*Prnp*$^{-/-}$ (ZrchI) brain were analyzed by Western blot analysis. The brain sample (60 μg) was separated by 12% SDS–PAGE, transferred onto a polyvinylidene difluoride (PVDF) membrane, and immunostained with anti-PrP 6H4 or anti-PrPLP/Dpl DDC39. The presence of PrP^C in brain homogenate of *Prnp*$^{+/+}$ mice and PrPLP/Dpl in brain homogenate of Rikn *Prnp*$^{-/-}$ mice was confirmed. (B,C) Copper (B) and manganese (C) levels were measured in brains of *Prnp*$^{+/+}$ (WT), Rikn *Prnp*$^{-/-}$, and FVB/*Prnp*$^{-/-}$ (ZrchI) mice by GF-AAS. Metal levels are given as μg/g dry weight. Differences where $p < 0.05$ (*) in copper concentration between *Prnp*$^{+/+}$ brain and Rikn *Prnp*$^{-/-}$ mouse brains were considered statistically significant.

In this study, cellular copper concentration was decreased in the absence of PrP^C under oxidative conditions. As serum deprivation increased production of superoxide anion which is reduced by re-introduction of *Prnp* in HpL3-4 cells [21], cellular copper concentration might be decreased by oxidative stress (PrP^C may stabilize cellular copper homeostasis possibly due to its antioxidant properties). To our knowledge, this is the first report that cellular copper concentration is decreased under oxidative conditions in the absence of PrP^C. Copper ion is a redox active metal that plays important catalytic roles in enzymes [29]. Moreover, as copper ion easily reacts with reactive oxygen species (ROS) and can generate free radicals [30], copper levels must be regulated to prevent aberrant reaction with ROS. Therefore, cellular copper concentration may be strictly regulated under oxidative conditions. Our previous studies have shown that PrP^C eliminates superoxide via the regulation of SOD activity [21]. Therefore, to elucidate the mechanism of copper homeostasis regulation by PrP^C, further studies on the relationship between copper homeostasis regulation and the antioxidative property of PrP^C are warranted. Our study also indicated that the stabilization of copper homeostasis by PrP^C was completely inhibited by overexpression of PrPLP/Dpl, which inhibited regulation of copper homeostasis by PrP^C in a dose-dependent manner. PrPLP/Dpl did not affect copper homeostasis in the absence of PrP^C. This suggests a potential interaction between PrP^C and PrPLP/Dpl. PrP^C has an affinity constant for copper in the micromolar range [31]. Copper bound to PrP^C is exchangeable to serum albumin and amino acids but not to ceruloplasmin within the physiological concentration range of the total copper concentration in plasma [31]. Therefore, PrP^C may play a role in transferring copper from serum albumin and amino acids in serum, and the transfer may be inhibited by overexpression of PrPLP/Dpl. In other cases, as PrPLP/Dpl may bind to copper in a manner similar to PrP^C [16], an alterative possibility could be proposed that PrP^C may not intracellularly transfer copper in the presence of PrPLP/Dpl due to the chelating effect of PrPLP/Dpl on copper. A dose-dependent influence of the expression of PrPLP/Dpl in increasing cellular manganese levels is also evidenced. These results indicate PrP^C has different roles in regulating metal homeostasis from PrPLP/Dpl, despite the homology of PrPLP/Dpl with PrP^C. Different sequences between PrP^C and PrPLP/Dpl would determine the discrimination of metal regulation. Manganese exists in non-transferrin-bound and transferrin-bound forms in the serum and extracellular fluid of the brain [32]. Although the non-transferrin-mediated pathway remains unclear, transferrin-bound manganese is taken up by cells via the transferrin receptor-mediated endocytosis [32]. As PrPLP/Dpl may not bind to manganese [16], PrPLP/Dpl may indirectly regulate manganese homeostasis by enhancing the endocytosis. An alternative possibility is that it may result from a secondary effect of the upregulation of manganese-containing proteins such as manganese-superoxide dismutase. We also demonstrated the combination of a lack of PrP^C and ectopic expression of PrPLP/Dpl decreased copper content in the mouse brain. Similarly, amyloid precursor protein (APP) contains metal binding sites for copper and zinc, and APP-knockout mice are reported to show elevations in brain and liver copper levels [33]. Additionally, we show that PrPLP/Dpl expression level-related increased in cellular manganese concentration, whereas ectopic expression of PrPLP/Dpl did not increase manganese content in the mouse brain. These results suggest that some cell populations or regions of the brain may regulate cellular manganese

concentration by PrPLP/Dpl expression, while other cell populations or regions of the brain may not. Therefore, further studies of the various cell types and dissected subregions of the brain in these mouse lines are needed to confirm possible cell type and region-specific alterations in manganese levels. Brains of Rcm0 *Prnp*$^{-/-}$ mice ectopically expressing PrPLP/Dpl show much higher levels of protein oxidation and lipid peroxidation than those of *Prnp*$^{+/+}$ mice or Npu *Prnp*$^{-/-}$ mice not ectopically expressing PrPLP/Dpl [18], suggesting that PrPLP/Dpl expression increases oxidative stress. This report and our results advocate that ectopic expression of PrPLP/Dpl in the absence of PrP^{C} decreases copper concentration in the brain with accompanying increased oxidative stress.

Prion diseases are thought to be due to the combined effect of an accumulation of an abnormal isoform of prion protein (PrP^{Sc}) and a deficiency of PrP^{C} in neurons [22]. PrP^{Sc} is derived from PrP^{C} [34]. This conversion leads to PrP^{Sc} accumulation and PrP^{C} deficiency in neurons [34]. The former causes oxidative stress in the animal brain [8,10]. Furthermore, neurons lacking PrP^{C} are susceptible to oxidative stress [35]. Therefore, the oxidative stress and lack of PrP^{C} caused by PrP^{Sc} may result in a loss of neurons. Recently, brains of scrapie-infected mice have been reported to show decreased copper levels prior to the onset of clinical symptoms [36]. Interestingly, in the present study, we found that Rikn *Prnp*$^{-/-}$ mice showed a decrease of copper levels compared to *Prnp*$^{+/+}$ mice, suggesting that Rikn *Prnp*$^{-/-}$ mice resemble scrapie-infected *Prnp*$^{+/+}$ mice in terms of metal homeostasis. Rikn *Prnp*$^{-/-}$ mice may be a useful model for studying the pathogenesis of neurodegenerative diseases accompanied by aberrant metal homeostasis such as prion diseases and Alzheimer's disease. Furthermore, it suggests that inhibition of oxidative stress and perturbation of copper homeostasis by pharmacological agents would be useful for a therapeutic approach for prion diseases.

Acknowledgments

We thank Dr. Stanley B. Prusiner (Institute for Neurodegenerative Diseases and Departments of Neurology and of Biochemistry and Biophysics, University of California) for providing FVB/*Prnp*$^{-/-}$ (ZrchI) mice. The authors are grateful to Dr. Anthony Foong for reading the manuscript. This work was supported by Grant-in-Aid from the Ministry of Health, Labour and Welfare of Japan (to K.S. and T.O.), Grant-in-Aid for Scientific Research on Priority Areas (to K.S.), and Grant-in-Aid for Scientific Research (to K.S. and T.O.) from the Ministry of Education, Science, Culture and Technology of Japan.

References

[1] M.P. Hornshaw, J.R. McDermott, J.M. Candy, Copper binding to the N-terminal tandem repeat regions of mammalian and avian prion protein, Biochem. Biophys. Res. Commun. 207 (1995) 621–629.

[2] D.R. Brown, K. Qin, J.W. Herms, A. Madlung, J. Manson, R. Strome, P.E. Fraser, T. Kruck, A. von Bohlen, W. Schulz-Schaeffer, A. Giese, D. Westaway, H. Kretzschmar, The cellular prion protein binds copper in vivo, Nature 390 (1997) 684–687.

[3] J.H. Viles, F.E. Cohen, S.B. Prusiner, D.B. Goodin, P.E. Wright, H.J. Dyson, Copper binding to the prion protein: structural implications of four identical cooperative binding sites, Proc. Natl. Acad. Sci. USA 96 (1999) 2042–2047.

[4] T. Miura, A. Hori-i, H. Mototani, H. Takeuchi, Raman spectroscopic study on the copper(II) binding mode of prion octapeptide and its pH dependence, Biochemistry 38 (1999) 11560–11569.

[5] M.L. Kramer, H.D. Kratzin, B. Schmidt, A. Romer, O. Windl, S. Liemann, S. Hornemann, H. Kretzschmar, Prion protein binds copper within the physiological concentration range, J. Biol. Chem. 276 (2001) 16711–16719.

[6] D.R. Brown, B.S. Wong, F. Hafiz, C. Clive, S.J. Haswell, I.M. Jones, Normal prion protein has an activity like that of superoxide dismutase, Biochem. J. 344 (1999) 1–5.

[7] D.R. Brown, F. Hafiz, L.L. Glasssmith, B.S. Wong, I.M. Jones, C. Clive, S.J. Haswell, Consequences of manganese replacement of copper for prion protein function and proteinase resistance, EMBO J. 19 (2000) 1180–1186.

[8] B.S. Wong, D.R. Brown, T. Pan, M. Whiteman, T. Liu, X. Bu, R. Li, P. Gambetti, J. Olesik, R. Rubenstein, M.S. Sy, Oxidative impairment in scrapie-infected mice is associated with brain metals perturbations and altered antioxidant activities, J. Neurochem. 79 (2001) 689–698.

[9] B.S. Wong, S.G. Chen, M. Colucci, Z. Xie, T. Pan, T. Liu, R. Li, P. Gambetti, M.S. Sy, D.R. Brown, Aberrant metal binding by prion protein in human prion disease, J. Neurochem. 78 (2001) 1400–1408.

[10] S.I. Choi, W.K. Ju, E.K. Choi, J. Kim, H.Z. Lea, R.I. Carp, H.M. Wisniewski, Y.S. Kim, Mitochondrial dysfunction induced by oxidative stress in the brains of hamsters infected with the 263K scrapie agent, Acta Neuropathol. (Berl) 96 (1998) 279–286.

[11] R.C. Moore, I.Y. Lee, G.L. Silverman, P.M. Harrison, R. Strome, C. Heinrich, A. Karunaratne, S.H. Pasternak, M.A. Chishti, Y. Liang, P. Mastrangelo, K. Wang, A.F. Smit, S. Katamine, G.A. Carlson, F.E. Cohen, S.B. Prusiner, D.W. Melton, P. Tremblay, L.E. Hood, D. Westaway, Ataxia in prion protein (PrP)-deficient mice is associated with upregulation of the novel PrP-like protein doppel, J. Mol. Biol. 292 (1999) 797–817.

[12] A. Li, S. Sakaguchi, R. Atarashi, B.C. Roy, R. Nakaoke, K. Arima, N. Okimura, J. Kopacek, K. Shigematsu, Identification of a novel gene encoding a PrP-like protein expressed as chimeric transcripts fused to PrP exon 1/2 in ataxic mouse line with a disrupted PrP gene, Cell. Mol. Neurobiol. 20 (2000) 553–567.

[13] N. Nishida, P. Tremblay, T. Sugimoto, K. Shigematsu, S. Shirabe, C. Petromilli, S.P. Erpel, R. Nakaoke, R. Atarashi, T. Houtani, M. Torchia, S. Sakaguchi, S.J. DeArmond, S.B. Prusiner, S. Katamine, A mouse prion protein transgene rescues mice deficient for the prion protein gene from purkinje cell degeneration and demyelination, Lab. Invest. 79 (1999) 689–697.

[14] D. Rossi, A. Cozzio, E. Flechsig, M.A. Klein, T. Rulicke, A. Aguzzi, C. Weissmann, Onset of ataxia and Purkinje cell loss in PrP null mice inversely correlated with Dpl level in brain, EMBO J. 20 (2001) 694–702.

[15] H. Mo, R.C. Moore, F.E. Cohen, D. Westaway, S.B. Prusiner, P.E. Wright, H.J. Dyson, Two different neurodegenerative diseases caused by proteins with similar structures, Proc. Natl. Acad. Sci. USA 98 (2001) 2352–2357.

[16] K. Qin, J. Coomaraswamy, P. Mastrangelo, Y. Yang, S. Lugowski, C. Petromilli, S.B. Prusiner, P.E. Fraser, J.M. Goldberg, A. Chakrabartty, D. Westaway, The PrP-like protein Doppel binds copper, J. Biol. Chem. 278 (2003) 8888–8896.

[17] Y. Shaked, N. Hijazi, R. Gabizon, Doppel and PrP(C) do not share the same membrane microenvironment, FEBS Lett. 530 (2002) 85–88.
[18] B.S. Wong, T. Liu, D. Paisley, R. Li, T. Pan, S.G. Chen, G. Perry, R.B. Petersen, M.A. Smith, D.W. Melton, P. Gambetti, D.R. Brown, M.S. Sy, Induction of HO-1 and NOS in doppel-expressing mice devoid of PrP: implications for doppel function, Mol. Cell. Neurosci. 17 (2001) 768–775.
[19] D.J. Waggoner, B. Drisaldi, T.B. Bartnikas, R.L. Casareno, J.R. Prohaska, J.D. Gitlin, D.A. Harris, Brain copper content and cuproenzyme activity do not vary with prion protein expression level, J. Biol. Chem. 275 (2000) 7455–7458.
[20] C. Kuwahara, A.M. Takeuchi, T. Nishimura, K. Haraguchi, A. Kubosaki, Y. Matsumoto, K. Saeki, T. Yokoyama, S. Itohara, T. Onodera, Prions prevent neuronal cell-line death, Nature 400 (1999) 225–226.
[21] A. Sakudo, D.C. Lee, K. Saeki, Y. Nakamura, K. Inoue, Y. Matsumoto, S. Itohara, T. Onodera, Impairment of superoxide dismutase activation by N-terminally truncated prion protein (PrP) in PrP-deficient neuronal cell line, Biochem. Biophys. Res. Commun. 308 (2003) 660–667.
[22] T. Yokoyama, K.M. Kimura, Y. Ushiki, S. Yamada, A. Morooka, T. Nakashiba, T. Sassa, S. Itohara, In vivo conversion of cellular prion protein to pathogenic isoforms, as monitored by conformation-specific antibodies, J. Biol. Chem. 276 (2001) 11265–11271.
[23] M. Kozak, An analysis of 5'-noncoding sequences from 699 vertebrate messenger RNAs, Nucleic Acids Res. 15 (1987) 8125–8148.
[24] K. Peoc'h, C. Serres, Y. Frobert, C. Martin, S. Lehmann, S. Chasseigneaux, V. Sazdovitch, J. Grassi, P. Jouannet, J.M. Launay, J.L. Laplanche, The human "prion-like" protein Doppel is expressed in both Sertoli cells and spermatozoa, J. Biol. Chem. 277 (2002) 43071–43078.
[25] C. Korth, B. Stierli, P. Streit, M. Moser, O. Schaller, R. Fischer, W. Schulz-Schaeffer, H. Kretzschmar, A. Raeber, U. Braun, F. Ehrensperger, S. Hornemann, R. Glockshuber, R. Riek, M. Billeter, K. Wuthrich, B. Oesch, Prion (PrPSc)-specific epitope defined by a monoclonal antibody, Nature 390 (1997) 74–77.
[26] I. Kojima, C. Iida, Vapor phase digestion of botanical samples with acids in sealed polytetrafluoroethylene bomb, Anal. Sci. 2 (1986) 567–570.
[27] C.J. Maynard, R. Cappai, I. Volitakis, R.A. Cherny, A.R. White, K. Beyreuther, C.L. Masters, A.I. Bush, Q.X. Li, Overexpression of Alzheimer's disease amyloid-beta opposes the age-dependent elevations of brain copper and iron, J. Biol. Chem. 277 (2002) 44670–44676.
[28] J.R. Prohaska, W.R. Bailey, Persistent regional changes in brain copper, cuproenzymes and catecholamines following perinatal copper deficiency in mice, J. Nutr. 123 (1993) 1226–1234.
[29] A.I. Bush, Metals and neuroscience, Curr. Opin. Chem. Biol. 4 (2000) 184–191.
[30] M.R. Gunther, P.M. Hanna, R.P. Mason, M.S. Cohen, Hydroxyl radical formation from cuprous ion and hydrogen peroxide: a spin-trapping study, Arch. Biochem. Biophys. 316 (1995) 515–522.
[31] S. Lehmann, Metal ions and prion diseases, Curr. Opin. Chem. Biol. 6 (2002) 187–192.
[32] A. Takeda, Manganese action in brain function, Brain Res. Brain Res. Rev. 41 (2003) 79–87.
[33] A.R. White, R. Reyes, J.F. Mercer, J. Camakaris, H. Zheng, A.I. Bush, G. Multhaup, K. Beyreuther, C.L. Masters, R. Cappai, Copper levels are increased in the cerebral cortex and liver of APP and APLP2 knockout mice, Brain Res. 842 (1999) 439–444.
[34] S.B. Prusiner, Prions, Proc. Natl. Acad. Sci. USA 95 (1998) 13363–13383.
[35] D.R. Brown, W.J. Schulz-Schaeffer, B. Schmidt, H.A. Kretzschmar, Prion protein-deficient cells show altered response to oxidative stress due to decreased SOD-1 activity, Exp. Neurol. 146 (1997) 104–112.
[36] A.M. Thackray, R. Knight, S.J. Haswell, R. Bujdoso, D.R. Brown, Metal imbalance and compromised antioxidant function are early changes in prion disease, Biochem. J. 362 (2002) 253–258.